Sodium and lithium incorporated cathode materials for energy storage applications - A focused review

Jeffin James Abraham [a], Christian Randell A. Arro [a], Hanan Abdurehman Tariq [a], Ramazan Kahraman [b], Siham Al-Qaradawi [c], Talal Mohammed Al tahtamouni [d], R.A. Shakoor [a],*

[a] Center for Advanced Materials (CAM), Qatar University, P. O. Box 2713, Doha, Qatar
[b] Department of Chemical Engineering, College of Engineering, Qatar University, P. O. Box 2713, Doha, Qatar
[c] Department of Chemistry & Earth Sciences, College of Arts and Science (CAS), Qatar University, P. O. Box 2713, Doha, Qatar
[d] Materials Science and Technology Master Program, College of Arts and Science (CAS), Qatar University, P. O. Box 2713, Doha, Qatar

HIGHLIGHTS

- A review on Na/Li incorporation in various cathodes is presented.
- Na/Li insertion affects the electrochemical performance of cathodes.
- Na addition increases structural stabilization in Li-based cathodes.
- Li addition limits phase transformation at high voltage in Na-based cathodes.

ARTICLE INFO

ABSTRACT

The idea of lithium (Li)/sodium (Na) incorporated cathodes for both Li/Na-ion batteries has gained significant consideration throughout the past decade. The encouraging performance of various reported Li/Na incorporated cathode systems has the potential to review their exciting developments made so far to clearly understand the effect of numerous variables in improving the electrochemical performance. The current manuscript provides a focused review on the synthesis and electrochemical performance of these Li/Na incorporated cathode materials for Na/Li-ion batteries. Furthermore, the ruling mechanisms affecting the electrochemical performance of Li/Na incorporated cathode materials have been summarized. The majority of the synthesized Li/Na incorporated cathodes demonstrate good electrochemical cyclic stability, capacity retention, rate capability, charge/discharge capacity, etc. Li incorporated Na-based cathodes, show improved performance that can be attributed to the prevention of phase transformation at high voltages and loss of transition metal from the cathode. In the case of Na addition to Li-based cathodes, the Na pillaring effect significantly improves the Li interface layer stability, increases Li-ion diffusion, and retardation of Li and/or transition metal disordering. Various factors affecting the performance of Li/Na incorporated cathode families have been discussed that can be taken into account for development of future novel cathode materials demonstrating decent performance.

1. Introduction

Energy is an integral part of every healthy economy. Throughout the past decades, energy was mostly utilized in the form of non-renewable fossil fuels as power sources. With depleting fossil fuel reserves, there has been an increased interest in renewable energy sources like solar, hydrothermal, wind energy, etc. [1–7]. However, usage of these renewable sources usually comes with proper energy storage requirements like batteries and supercapacitors. Battery operation dramatically relies on the electrodes in redox reactions and has reasonable operating voltages compared to supercapacitors [8–15]. The electrode materials used in batteries profoundly influence the capacity of the batteries due to various factors. One such factor is the crystal lattice of the electrode material, which needs to provide ion exchange locations at the time of charge/discharge. Nevertheless, this is also considered as a disadvantage because solid-state mass diffusion can

impede the idea of fast charging [16]. Various types of batteries have been developed throughout the years, and one of the most commonly used battery technologies is the Lithium (Li) ion battery. These batteries are used in many different electronic devices such as laptops, mobile phones, and recently even deployed for use in electric vehicles (EVs) and hybrid electric vehicles (HEVs) [17]. Due to high energy efficiency, these Li-ion batteries can further be used in energy storage applications from renewable sources of energy like solar, wind, and geothermal energy [18]. The current Li-ion battery technology has been commercialized to a massive extent. Many large scale energy storage systems have tested the viability of Li-ion batteries for stationary applications. However, the use of Li-ion batteries has also met with some resistance due to Li's costly nature, lack of Li reserves in the world, and the use of some hazardous transition metals in Li electrodes [19]. The high kWh price is an important barrier to the large scale use of Li ion in stationary applications. Therefore, after many years of research, Sodium (Na) ion batteries were developed as an alternative to Li-ion batteries. Many different metals have been tested to serve as the cathode materials in batteries, however very few are suitable.

Na-ion batteries work on a similar principle as Li-ion batteries and display similar energy storage properties as Li-ion batteries. Its abundance, cost efficiency, and considerable capacity make it a viable alternative to Li-ion batteries [20,21]. Table 1 gives a brief insight into the characteristics of both Na and Li materials, as reported by Palomares et al. [22]. The usage of Na instead of Li can help in the development of cheaper Na-ion batteries because Na has a higher half-reaction potential compared to Li and thus can be used in lower decomposition potential electrolyte systems [22]. It has been recently reported that cost of Na-ion batteries are on average 10–20% lower than of Li-ion batteries [23]. Na-ion batteries and Li-ion batteries have certain similarities, such as identical synthesis, characterization, and analysis techniques, enabling an easier understanding of Na-ion battery development fundamentals. Furthermore, Na displays a redox potential of $E^{\circ}_{(Na^+/Na)}$ of -2.71 V vs. the standard hydrogen electrode (SHE) compared to the redox potential of $Li - E^{\circ}_{(Li^+/Li)}$ of -3.0 V vs. SHE [24]. Na-ion batteries also have demerits compared to Li-ion batteries, as these show more inadequate energy densities [23]. The main disadvantages of using Na-ion battery comes in the form factor of poor power and energy density as compared to the Li-ion battery technology, lack of stable intercalation materials and therefore shorter lifetime. As both Na-ion and Li-ion battery still display a lack of high energy and power density, there is a requirement to develop new cathode materials, based on non-scarce materials and produced via green chemistry routes, having improved performance to meet the growing needs of the society.

Both Li-ion and Na-ion batteries have their advantages and disadvantages, and various strategies have been designed to improve their performance further and negate the disadvantages. One such technique is incorporating either Li metal into a Na based cathodes or a Na metal into a Li based cathodes, commonly known through terms like Li/Na doped or substituted cathode materials formation. The incorporation of Li/Na in Na/Li ion battery cathode materials has been considered a viable strategy by various researchers [25–28]. The use of both Na and Li incorporated cathodes has been developed to integrate Na and Li
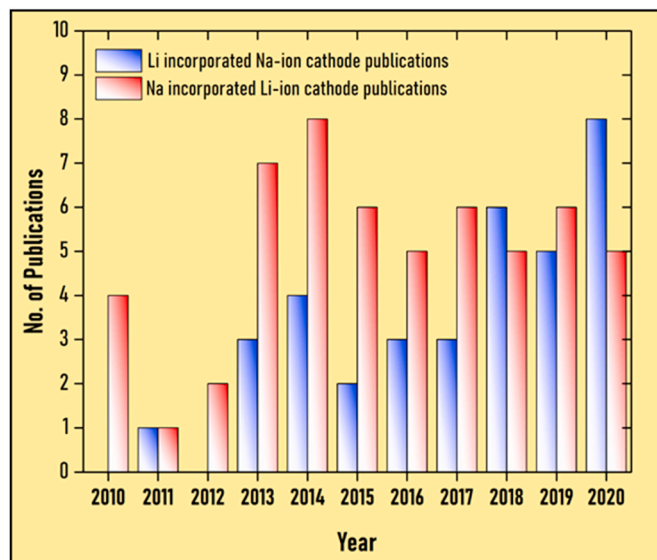
technology's outstanding advantages. Moreover, understanding of the intercalation/de-intercalation mechanism has enabled to understand the reason for improved performance clearly. Throughout the past decade, there have been various studies into these types of cathode materials. Fig. 1 shows the number of publications per year on the topic of Na/Li incorporated cathode materials. Unlike other cathode materials, the literature on these cathode materials is not rich enough. However, several reports have been published and the number of reports on this topic have been increasing throughout the years. The increasing number of publications on this topic per year suggest a positive trend on this field of cathode materials for future battery storage technology. Here in this review, we compile a list of reported cathode materials that use both Li and Na in their batteries. Moreover, various synthesis techniques reported for the development of these cathodes and their electrochemical performance have been summarized. Finally, a comprehensive comparative analysis is conducted to precisely review and understand the effect of the synthesis technique on the performance of these cathode materials. The majority of the synthesized cathodes demonstrate good electrochemical cyclic stability, capacity retention, rate capability, charge/discharge capacity, etc. Li incorporated Na-ion battery cathodes, show improved performance that can be attributed to the prevention of phase transformation at high voltages and loss of transition metal from the cathode. In Na's case to Li-ion battery cathodes, the Na pillaring effect improves the Li interface layer stability, increases Li-ion diffusion, and limits Li and/or transition metal disordering. Development of these Li/Na incorporated cathode materials, acting as building blocks, can help in future development of various smart materials or electromagnetic composites [29–33]. A clear understanding of the governing mechanism may lead to developing some novel and promising cathode materials demonstrating enhanced electrochemical performance for future energy storage applications.

2. Li incorporated Na-based cathode materials

2.1. Na-based oxide cathodes

2.1.1. P2-type oxide cathode materials

2.1.1.1. Manganese rich oxide cathodes.
Perhaps one of the most common Li incorporated cathodes in Na-ion batteries are the oxide type. There have been multiple reports of Li incorporation through doping or

Table 1
A list of characteristics for Li and Na metals. Reproduced from Energy Environment Science, 5, V. Palomares, P. Serras, I. Villaluenga, K.B. Hueso, J. Carretero-González, T. Rojo, Na-ion batteries, recent advances and present challenges to become low cost energy storage systems, 5884–5901, with permission from The Royal Society of Chemistry [22].

Characteristics	Li	Na
Price	4.11–4.49€Kg^{-1}	0.07–0.37€Kg^{-1}
Ionic radius	0.69 Å	0.98 Å
Melting point	180.5 °C	97.7 °C
Capacity density	3.86 Ahg^{-1}	1.16 Ahg^{-1}

Fig. 1. List of publications on Na/Li incorporated cathodes throughout the past decade.

substitution in P2-type structure and O3-type structure of Na-ion oxide-based cathodes. The P2-type Na layered oxides are significant as battery cathodes, mainly due to their unique structure, broad diffusion paths, and structural stability, and a better structure that accommodates Na^+ ions easily [34,35]. The earliest report, as to our knowledge, for Li-substituted sodium-based oxide cathode for Na-ion battery is from Kim et al. [25] associated to the layered oxide type material $Na_xLi_yNi_{0.25}Mn_{0.75}O_\delta$ ($0.7 \leq x \leq 1.2$; $0 < y \leq 0.5$). The Kim group synthesized phase pure $Na_{1.0}Li_{0.2}Ni_{0.25}Mn_{0.75}O_\delta$ material using the conventional powder metallurgy route followed by sintering the precursor materials at high temperature in air. The material composition was chosen to keep the stability of the cathode material. Li metal was incorporated as a part of the transition metal layer considering stabilization of charge ordering state between manganese (IV) and nickel (II) [25]. The synthesized cathode material contains Mn^{4+} and Ni^{2+}. For the stability of the developed structure, an oxygen-rich material, $\delta > 2.2$ was required, hence by normalizing the material in terms of O^{2-}, the final synthesized product phase deficient in Na was $Na_{0.85}Li_{0.17}Ni_{0.21}Mn_{0.64}O_2$. The theoretical capacity of the as-synthesized cathode material is 112 mAhg^{-1} and had a testing capacity is 95–100 mAhg^{-1}, which is 87% of the theoretical capacity throughout a course of 50 cycles at 15 mAg^{-1} rate [25]. The alkali layer only contained Na in trigonal prismatic coordination whereas the transition metal layer contained, Ni (II), Mn(IV) and Li with the octahedral coordination and the metal layer showed less than 1% structural volume change during cycling, staying intact through the cycling process. With both Mn in +4 oxidation state and Ni in +2 oxidation state, there is a lack of Jahn-Teller octahedral distortion. The presence of Li in the transition metal layer of this material prevents Ni from entering the alkali layer during the deintercalation/intercalation of Na from the crystal structure. The development of this electrode by the Kim group was a forward step in the development of future Li incorporated cathodes by many other groups.

The P2-type-Na_2MO_3 (M-transition metal) is a promising cathode material reported previously [36–38]. However, Na_2MnO_3 suffers from low capacity compared to its Li counterpart, Li_2MnO_3, mainly due to the ionic radii difference between Na^+ (1.02 Å) and Mn^{4+} (0.53 Å). The presence of oxide ions results in the activation of manganese ions and is beneficial for the redox reaction leading to high capacities for Li_2MnO_3 based cathodes [39]. Yabuuchi et al. [40] reported a P2-type cathode in Na cell $Na_{5/6}[Li_{1/4}Mn_{3/4}]O_2$, and De La Llave et al. [39] reported a P2-$Na_{0.6}Li_{0.2}Mn_{0.8}O_2$ cathode material where Mn is in the Mn^{4+} oxidation state and the material is analogous to Li_2MnO_3 cathode material, having similar structure and electrochemical performance. $Na_{5/6}[Li_{1/4}Mn_{3/4}]O_2$ was synthesized by the conventional solid-state reaction technique [40], and $Na_{0.6}Li_{0.2}Mn_{0.8}O_2$ cathode material was developed by self-combustion reactions (SCR) [41]. $Na_{5/6}[Li_{1/4}Mn_{3/4}]O_2$ demonstrates a capacity of ~200 mAhg^{-1} at 10 mAg^{-1} rate and with good capacity retention up to 20 cycles. Similarly, $Na_{0.6}Li_{0.2}Mn_{0.8}O_2$ also exhibits a capacity of ~190 mAhg^{-1} at 12 mAg^{-1} current density and stable performance for 100 cycles [39,40]. The introduction of Lithium ions as a substituent to sodium stabilizes the structure of both $Na_{5/6}[Li_{1/4}Mn_{3/4}]O_2$ and $Na_{0.6}Li_{0.2}Mn_{0.8}O_2$ as reported by their stable electrochemical performance. When charged to 4.4 V the Li^+ ions which are predominantly present in the transition metal layer traverses to the Na alkali layer and on discharge return to their transition metal layer sites. There is lithium extraction from the transition metal layer and partial oxygen loss, which results in in-plane cation rearrangements, which considerably improves the reversible capacity of the materials. This also activates the Mn^{4+} ions in the Na cell of these materials. Through Li substitution in the Mn rich materials, there is an increase in operating voltages of the materials and it affects phase transition mechanism whether it is a single-phase reaction, two-phase separation or a miscibility gap [40]. The incorporation of Lithium limits the destructive P2 phase transitions of these cathode materials at high voltage potentials during charging and further reduces the occurring of Jahn-Teller distortions [39,40].

The Na layered cathode materials display phase transformations during electrochemical testing resulting in multiple voltage steps in their electrochemical profile and various challenges such as inferior rate capabilities and shortened cycle life [42–45]. Xu et al. [34] synthesized P2-$Na_x[Li_yNi_zMn_{1-y-z}]O_2$ ($0 < x, y, z < 1$) Li substituted cathode material by a co-precipitation technique using transition metal nitrates as the reactants. The identified stoichiometry of the synthesized material was $Na_{0.80}[Li_{0.12}Ni_{0.22}Mn_{0.66}]O_2$. The theoretical capacity of the synthesized cathode material is 118 mAhg^{-1}. During cycling, it displayed a reversible capacity of 115 mAhg^{-1} with a capacity retention of 91% for 50 cycles. It is observed in the rate capability data that $Na_{0.80}[Li_{0.12}Ni_{0.22}Mn_{0.66}]O_2$ cathode material shows a capacity of 70 mAhg^{-1} at 5C rate suggesting capacity stabilization at high C rates due to Li insertion. Furthermore, the voltage profile reveals a single-phase reaction during the charge/discharge process in the voltage range 2.0–4.4 V compared to the multiple phase transformations observed in P2-$Na_{2/3}[Ni_{1/3}Mn_{2/3}]O_2$, form 2.0–4.5 V, confirming a positive effect from Li insertion into P2-type cathode material [34,45]. Through nuclear magnetic resonance (NMR) and neutron diffraction, Xu et al. [34] were able to identify that the Li-ion predominantly appears in the transition metal sites, likely replacing Ni^{2+} ions and positioning closest to a high number of Mn^{4+} ions. During deintercalation, the cathode material experiences stacking faults from 4.1 V to 4.4 V range due to removal of the Na ions and during intercalation, these stacking faults are removed when the Na sites are rebuilt [34]. These stacking faults facilitate Li ion movement from the transition metal layer to the alkali layer, octahedral or tetrahedral sites. The reasoning for this material's excellent capacity and voltage curves showing a single-phase transformation is mainly due to the excellent Li migration reversibility.

2.1.1.2. Mn-M doped oxide cathodes (M → Fe, Ti). The Mn rich oxide cathode materials tend to have a positive effect on the redox reaction of the Na-ion layered oxide cathodes materials. However, it also has adverse effects like low structural stability and phase transition at high voltage [46,47]. There is a phase transition from the P2–O2 during high voltage testing, which results in the degeneration of the cathode. However, Li doping prevents P2–O2 transition by stabilizing the oxygen layer and prevents deformation with the help of high valent Mn^{4+} ions [48]. However, there is a significant loss in Lithium during the cycling process resulting in capacity decay. For structural stabilization during long term cycling, the key is to have Lithium stay in the transition metal layer [49]. The addition of iron (Fe) in the transition metal layer positively impacts the cathode structure as the high Fe^{3+}/Fe^{4+} redox voltage fixes Lithium in its lattice position during electrochemical tests [49]. Sodium-based iron-manganese oxides containing Lithium have also been considered as a potential cathode for Na-ion batteries. Ding et al. [46] reported a P2-$Na_{0.6}Li_{0.2}Fe_{0.2}Mn_{0.6}O_2$ cathode material synthesized by self-combustion reactions, and Yang et al. [49] reported a P2-$Na_{0.66}Li_{0.18}Fe_{0.12}Mn_{0.7}O_2$ cathode material synthesized using solid-state reaction technique. The $Na_{0.6}Li_{0.2}Fe_{0.2}Mn_{0.6}O_2$ cathode material displayed a reversible capacity of ~167 mAhg^{-1} at 0.2 C rate and capacity retention of 73% throughout 120 cycles. The XPS analysis of the material states a decrease in the oxidation state of Mn ions (Mn^{3+}) and an increase in Fe ions (Fe^{3+}) due to the presence of Li in the structure, thereby limiting Jahn-Teller distortions [46]. Fig. 2 shows the electrochemical characterization and performance of $Na_{0.66}Li_{0.18}Fe_{0.12}Mn_{0.7}O_2$ in Na half-cells. Fig. 2 (a,b) shows the charge-discharge curve and cyclability of the cathode material up to 80 cycles. The $Na_{0.66}Li_{0.18}Fe_{0.12}Mn_{0.7}O_2$ cathode displayed a stable capacity of ~165 mAhg^{-1} at a rate of 10 mAg^{-1} keeping capacity retention of 86.8% for 80 cycles. Even after 80 cycles, the material shows a columbic efficiency of 100% suggesting stable cycle life. Fig. 2(c) shows the cyclic voltammetry curves of the material at 0.1 mVs^{-1} rate. The first cycle is irreversible; hence, it shows two sharp and distinct peaks between 3.5 V and
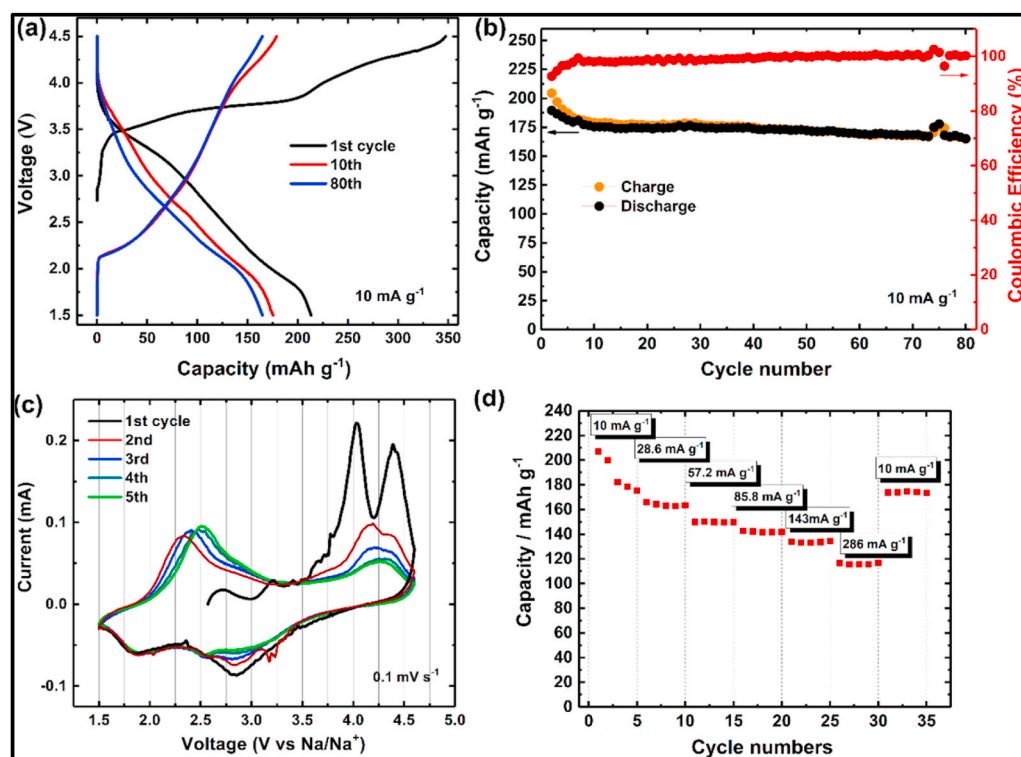
Fig. 2. Electrochemical performance of $Na_{0.66}Li_{0.18}Fe_{0.12}Mn_{0.7}O_2$ in Na half-cells: (a) galvanostatic charge/discharge curves (10 mAg^{-1}) - voltage range of 1.5–4.5 V, (b) cycling capacity and Columbic efficiency, (c) cyclic voltammetry curves - voltage range of 1.5–4.6 V, and (d) rate capability. Reprinted (adapted) with permission from Journal of American Chemical Society, 141, Yang, X. Li, J. Liu, S. Xiong, X. Ma, P. Liu, J. Bai, W. Xu, Y. Tang, Y.Y. Hu, M. Liu, H. Chen, Lithium-Doping Stabilized High-Performance P2-$Na_{0.66}Li_{0.18}Fe_{0.12}Mn_{0.7}O_2$ Cathode for Sodium Ion Batteries, 6680–6689. Copyright (2019) American Chemical Society [49].

4.5 V compared to the more blunt peaks in that range with the subsequent cycles. The rate capability data of the materials is reported in Fig. 2(d). Even at very high rates of 286 mAg^{-1}, the material continues to deliver a capacity of ~110 mAhg^{-1} and further shows capacity recoverability when re-cycled at 10 mAg^{-1}. The improved performance and stability of this material were attributed to factors such as the elimination of P2–O2 phase transition and negligible loss of Li from the lattice structure, proving the ability of Li and Fe doping in the host cathode structure [49]. There have been further reports on the improved effect of Li substitution as seen from the P2 type cathode materials like $Na_xLi_{0.25}Mn_{0.75}O_2$ (x = 0.75–0.833) [50], $Li_{0.2}Na_{1.0}Mn_{0.8}O_2$ [51], and $Na_{0.6}Li_{0.07}Mn_{0.66}Co_{0.17}Ni_{0.17}O_2$ [52]. These share the same principle of increased electrochemical performance due to Li substitution. The use of Titanium (Ti) and Li co-doping has been suggested recently as a technique for improved electrochemical performance. P2 type cathode materials like $Na_{0.8}(Li_{0.33}Mn_{0.67-x}Ti_x)O_2$ (x = 0, 0.05, 0.1 and 0.2) [53], and $Na_{0.560}[Li_{0.041}Mn_{0.642}Ni_{0.221}Ti_{0.095}]O_2$ [54] were tested and reported to have improved electrochemical performance due to Ti and Li Co-doping. The Mn in the cathode material during discharge changes from the 4+ oxidation to 3+ oxidation state. This adversely affects the performance and structural stability of the material by inducing Jahn teller structural distortion and dissolving the manganese [55]. The Ti present in the structure will limit the Mn^{3+} formation. Further studies by Ma et al. [53] confirms the lack of participation of Ti in the redox reaction, as Ti remains in Ti^{4+} oxidation state and limits Mn^{3+} formation slowing down the phase transitions improving performance. During deintercalation the Li in the transition metal layer moves to the alkali layer leaving vacancies inducing stress on the transition metal layers due to oxygen ion repulsions. The Ti in the material creates a Ti–O bond, having a stronger electrostatic attraction than the Ni–O and Mn–O bonds [56]. This stabilizes the structural slab of the cathode material, increasing stability, and the Li in the structure reduces the stress on the structural slabs caused during intercalation/deintercalation thereby increasing the electrochemical performance of the material [53,54].

2.1.2. O3-type

2.1.2.1. Ni–Mn–Co (NMC) oxide cathodes.
Like P2-type oxides, the O3-type oxide cathodes also display good electrochemical performance. O3-type cathodes like $NaNi_{0.5}Mn_{0.5}O_2$ [57], $NaTi_{0.5}Ni_{0.5}O_2$ [58], $NaVO_2$ [59] and $NaNi_{1/3}Mn_{1/3}Co_{1/3}O_2$ [60] have been reported. These cathodes demonstrate low reversible capacity (125 mAhg^{-1}) as compared to P2-type oxide cathodes [61–63]. While the P2-type oxide cathode displays a higher reversible capacity than the O3-type cathodes, it suffers from poor cyclability. In contrast, the O3-type cathodes display good cycle life compared to the P2-type but have a significantly lower capacity [64]. It is integral to design oxide cathodes having good cyclability and capacity. As discussed previously, one possible reported solution is the incorporation of Li in the structure of P2-type oxide cathodes to develop O3-type cathode materials for Na-ion batteries with improved cyclability. Xu et al. [65] prepared an NMC (Ni, Mn, Co) based O3-type cathode material ($NaLi_xNi_{1/3-x}Mn_{1/3+x}Co_{1/3-x}O_2$ (x = 0.07, 0.13, and 0.2) for Na-ion batteries. The cathode material was synthesized by a conventional co-precipitation method. Fig. 3(a–c) shows the XRD, crystal structure, and FE- SEM micrographs. Small impurity phase peaks are observed in the XRD data when the concentration of Li is increased to 0.13 and 0.2. Moreover, the structural arrangement of this material is the alkali layer and transition metal layer stacked in between two oxygen layers. The charge-discharge curves are seen in Fig. 3(d) up to 50 cycles, and the cyclability of the material is shown in Fig. 3(e). Phase pure $NaLi_{0.07}Ni_{0.26}Mn_{0.4}Co_{0.26}O_2$ cathode showed performance delivering a reversible capacity of ~110 mAhg^{-1} at a current density of 125 mAg^{-1} with a capacity retention of 98% throughout 50 cycles in the voltage range of 1.5–4.5 V [65]. Furthermore, the inset of Fig. 3(e) shows the discharge curves of the material at different rates. The reported performance of different concentrations of Li in this material suggested that 0.07 was the best concentration for this material and increasing the amount of Li in the material resulted in formation of new impurity phase as observed from the XRD data. The transition metals exist as Ni^{2+}, Co^{3+} and Mn^{4+} in the pristine material. In the NMC material, the main redox couple during cycling is Ni^{2+}/Ni^{4+} while the
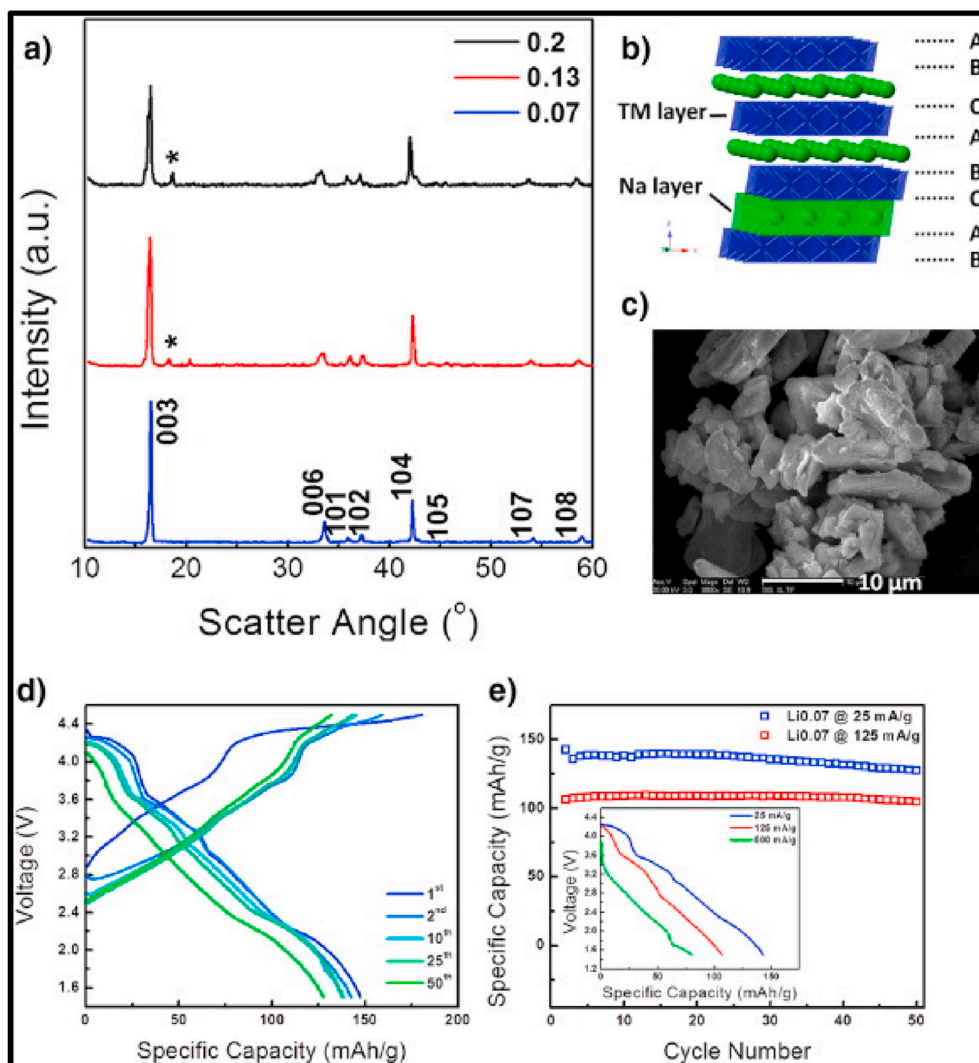
Fig. 3. $NaLi_{0.07}Ni_{0.26}Mn_{0.4}Co_{0.26}O_2$ cathode: (a) XRD, (b) crystal structure, (c) SEM, (d) galvanostatic charge-discharge curves, and (e) cycling data and inset (discharge curves at different C rates). Reprinted from Electrochemistry Communications, 60, J. Xu, H. Liu, Y.S. Meng, Exploring Li substituted O3-structured layered oxides $NaLi_xNi_{1/3-x}Mn_{1/3+x}Co_{1/3-x}O_2$ (x = 0.07, 0.13, and 0.2) as promising cathode materials for rechargeable Na batteries, 13–16, Copyright (2015), with permission from Elsevier [65].

Co^{3+}/Co^{4+} couple partly activates for charge balancing. The Mn has its main role in stabilizing the structure of the material during cycling mainly to prevent Jahn-Teller distortions from the Mn^{3+} ions. Other than the underlying role of Ni, Co and Mn, the Li substitution in the structure has very similar effects like prevention of phase transformation and structural stability as in the P2-type materials.

2.1.2.2. Cobalt free oxides. Cobalt (Co) free cathodes have been considered previously due to limited Co reserves and increasing price [66]. In this regard, Co-free Li incorporated Na-ion layered oxide cathode materials have also effectively worked as next generation battery solutions. Liu et al. [67] improved the layered oxide cathodes by designing a Co-free $O3–Na_{0.78}Li_{0.18}Ni_{0.25}Mn_{0.583}O_w$ cathode using the in-situ Li/Na-ion exchange process. For this purpose, $Li_{1.167}Ni_{0.25}Mn_{0.583}O_2$ was synthesized first and then charged in Li half-cell for Li extraction. The Li metal electrode is then replaced with Na metal and discharged in Na half-cell to obtain $O3–Na_{0.78}Li_{0.18}Ni_{0.25}Mn_{0.583}O_w$ [67]. The developed $O3–Na_{0.78}Li_{0.18}Ni_{0.25}Mn_{0.583}O_w$ cathode material displays an impressive discharge capacity of 240 mAhg^{-1} in the voltage window of 1.5–4.5 V. Moreover, it also exhibits a stable capacity retention of 190 mAhg^{-1} at the current density of 125 mAg^{-1} over a course of 30 cycles in the voltage window of 1.5–4.2 V. These results confirm the improved electrochemical performance (high reversible capacity, good capacity retention and cyclability) of $O3-Na_{0.78}Li_{0.18}Ni_{0.25}Mn_{0.583}O_w$ [67]. This developed material reported the highest reported discharge capacity among all the Na-ion materials. Since an ion-exchange synthesis method was utilized, the first discharge delithiates the sample, and then the sample is sodiated during charge using sodium metal anode. The first charge shifts the Li remaining in the structure to the tetrahedral sites, which actively plays the role as stabilizer during the remaining cycles of the material by preventing the neighbouring layers from shifting [67]. During the entire intercalation/deintercalation process, the oxidation state of Mn remains as Mn^{+4} whereas the Ni redox couple switches between Ni^{2+}/Ni^{4+} [65,67]. This is similar to that in the case of the NMC materials. The Li addition into the cathode structure improved performance of these cathodes indicating the stability of the lattice structure. Although this material displays outstanding electrochemical performance, its viability for commercialization is questioned owing to the complicated ion-exchange synthesis process.

2.1.2.3. Mn–Fe based oxide cathodes. The O3-type layered oxide cathodes' main issue is the phase transition to P3-P′3 occurring at high voltages and loss of transition metals during electrochemical testing [26, 67,68]. Identifying potential candidates for O3-type oxide cathodes is hard, and various materials from the Li counterpart have been considered for it. Out of these, the transition metal oxides Na_xMO_2, $0.67 < x \leq 1$; M: Mn, Ni, Fe, series have been considered for their potentially high theoretical capacity, adjustable voltage range, and lower cost [69–71]. However, the O3-type layered oxides display low voltage tolerance at

high voltages, V > 4.0 V, due to their unstable surface electrochemistry, eventually causing lower capacity and energy density [25,72–75]. During electrochemical testing, the crystal structure destabilizes due to distorted lattices and changes in volume resulting in multiphase transitions, which can further destabilize the cathode structure leading to poor performance. The electrolyte also used severely affects some of these cathodes. During electrochemical testing, the electrolytes like $NaPF_6$ (sodium hexafluorophosphate) and FEC (fluoroethylene carbonate), may decompose forming hydrogen fluoride (HF). As HF comes into contact with the layered oxide cathode, it can react with the transition metal ions forming transition metal fluorides [26,76]. The transition metal fluorides cause cathode mass loss creating barriers at the Solid Electrolyte Interface (SEI), reducing the flow of Na^+ ions during intercalation/deintercalation process. The NMF based cathode, where N: Ni, M: Mn, and F: Fe, is a promising cathode transition metal composition for O3 type layered oxide cathodes. Both Ni and Fe play an active role in the deterioration of the performance of the NMF based cathodes due to their active participation in the redox process at high voltages. There is a phase change from O3–P3 due to Jahn-Teller distortion of Ni^{3+} during cycling at high voltages. Further, there is the migration of Fe during cycling, which also affects the cathode's structural stability [26,77,78]. Oh et al. [77] synthesized an O3-type $Na[Li_{0.05}(Ni_{0.25}Fe_{0.25}Mn_{0.5})_{0.95}]O_2$ cathode material by actively doping Li in the transition metal layer and You et al. [26] developed an O3-type $Na_{0.85}Li_{0.1\text{-}}Ni_{0.175}Mn_{0.525}Fe_{0.2}O_2$ cathode by substituting Li for Na [26,77]. Both cathodes were synthesized by the co-precipitation process. The O3-type $Na[Li_{0.05}(Ni_{0.25}Fe_{0.25}Mn_{0.5})_{0.95}]O_2$ cathode shows a capacity of ~180 mAhg^{-1} at 0.1C rate. Moreover, when the cathode material is run in a full cell using hard carbon as an anode, it offers impressive capacity retention of 76% at a 0.5C rate for 200 cycles in the voltage range of 1.5–4.5 V [77]. The improved result can be attributed to Li's presence in the host structure, improving its stability by preventing Fe^{3+} migration to the Na layer. The O3-type $Na_{0.85}Li_{0.1}Ni_{0.175}Mn_{0.525}Fe_{0.2}O_2$ cathode material displays a capacity of ~160 mAhg^{-1} at 0.1C rate relatively high voltage of 4.5 V with a capacity retention of 88% at 1C rate for 100 cycles [26]. The high voltage stable performance is solely attributed to the incorporation of Li in the NMF structure. The Li is described to have a dual stabilization effect of limiting Jahn-Teller distortion and protecting the cathode-electrolyte interphase by bonding with the F^- anion, limiting the loss of active transition metal ions [26]. Recent studies by Wang et al. [79] reported the incorporation of Li in the alkali layer of $Na_x[Fe_yMn_{1\text{-}y}]O_2$ ($0 \leq x, y \leq 1$). The solid-state synthesis technique was employed for synthesis of this material. Out of all the compositions tested, $Na_{0.67}Li_{0.2}Fe_{0.4}Mn_{0.4}O_2$ showed the best electrochemical performance. This was mainly attributed to the fact that there was successful substitution of Li in the alkali layer of the parent material. The Li substitution in the resulting material shortens the interlayer distance, and improved electrochemical performance of the material. Comparatively to the pure material, the Li substituted material decreased the energy barrier required for Na diffusion mainly due to presence of Li in the alkali site which assists in pseudo-tetrahedral diffusion of Na [79].

2.1.3. Biphasic cathodes

Biphasic cathodes are materials that display properties of both P2 and O3 type oxides. Most of the reported Li incorporated oxide materials exist as either P2 type or O3 type oxide materials. In the case of P2 type cathode materials, they exhibit excellent electrochemical properties due to improved Na diffusion caused by face sharing trigonal prismatic sites present in the Na layer [25,80]. Most of the P2 phase oxide cathode materials are however, Na deficient causing decreased specific capacities [81]. In the case of the O3 type layered structure cathodes, the Na diffusion to the octahedral sites takes place through edge sharing of the tetrahedral sites [80]. The Na ions are unable to occupy the tetrahedral sites due to its size causing a high energy barrier [82]. This results in multi-phase transformations during electrochemical testing which destabilizes the structure decreasing electrochemical performance of the

material. Furthermore, during de-intercalation of O3 types materials, there is a phase transition from O3–P3 which causes energy loss due to high-energy barrier effect of the tetrahedral sites which is not present in P2–P3 phase transition for the P2 type materials [80]. To address the adverse effects related with both P2 and O3 type cathodes, a new P2/O3 Biphasic type Li incorporated Na ion cathode material has been recently proposed to combine the properties of P2 and O3 type oxide cathode material for increased capacity and cycling performance. The synthesized biphasic cathode material, $Na_{0.8}Li_{0.2}Fe_{0.2}Mn_{0.6}O_2$, was designed as Ni and Co free, which effectively lowers the cost of the Na-ion battery. The synthesis was done through sol-gel process and showed a mixed with 34% for P2 and 60% for O3 as well as a small secondary phase [83]. The transition metals Fe was in +3 oxidation state, and Mn was in +4 oxidation state. Moreover, 95% of the Li was located in the transition metal layer, and only 5% was in the alkali layer which leads to a more stable transition metal layer during Intercalation/deintercalation process [83]. Fig. 4 shows the electrochemical performance of the as-synthesized biphasic $Na_{0.8}Li_{0.2}Fe_{0.2}Mn_{0.6}O_2$ cathode material. The galvanostatic charge–discharge curves of up to 100 cycles is seen in Fig. 4(a) and the cyclability curve of the material is shown in Fig. 4(c) From a performance standpoint, the material delivered a capacity of 174 mAhg^{-1} and showed cyclic stability of up to 82% for 100 cycles at 0.1 C rate [83]. From charge/discharge voltage curves (Fig. 4(b)), a voltage decay is observed for the material over a course of 100 cycles. This is also conveyed through loss of energy density over the 100 cycles. It was also reported that a multiphase transition process occurs at different states of charge, with the most dominant phase being the O phase. However, the material was also was able to preserve its biphasic nature even after 30 cycles at a discharged state [83]. The rate capability data (Fig. 4(d)) also shows promising results for this biphasic material, showing a capacity of ~75 mAhg^{-1} at 3C rate suggesting improved performance and stability with addition of Li in the material. Other reported biphasic cathodes include $Na_{1\text{-}x}Li_xNi_{0.5}Mn_{0.5}O_{2+d}$ by Lee et al. [80] and. $Na_{0.66}Li_{0.18}Mn_{0.71}Ni_{0.21}Co_{0.08}O_{2+\delta}$ by Guo et al. [84]. Both groups reported the formation of multi-phase materials when Li is incorporated into the parent materials and improved electrochemical performance compared to the pristine materials. Through Li incorporation, the O3-$NaNi_{0.5}Mn_{0.5}O_2$ cathode material develops a P2 intergrowth and the P2-Na_xMnO_2 material develops an O3 intergrowth. The Li incorporation results in an intergrowth, which prevents layer shifting, thereby allowing smooth Na diffusion, and hence enhances the electrochemical performance of the materials. Development of such biphasic cathodes, displaying properties of both the P2 phase and O3 phase oxides is a promising step towards high energy and power density batteries.

2.2. Pyrophosphate

The Pyrophosphate family of cathode materials have been considered promising for next generation Na-ion batteries due to their stable crystal structure, low cost, and improved thermal properties resulting in improved safety [85–88]. Cathode materials like $Na_2FeP_2O_7$, $Na_2VP_2O_7$, and $Na_2Fe_{0.5}Mn_{0.5}P_2O_7$ are known for their excellent structural stability. However, these cathode materials lack energy density [87–89]. To address the challenges related to the pyrophosphate family of cathode materials, different techniques such as doping, coatings, particle size reduction, and transition metal substituting were reported [90–93]. Recently, Li incorporation in host structure of $Na_2FeP_2O_7$ material has been investigated [94]. The solid-state ball milling technique synthesized the Li-substituted cathode material ($Na_{1.4}Li_{0.6}FeP_2O_7$), and the X-ray diffraction (XRD) spectra confirms the phase purity of the material [94]. However, the expected improved performance was not observed in the case of the Na-ion battery. The Na half-cell of this cathode material demonstrates a capacity of ~65 mAhg^{-1} at 0.05C rate throughout 50 cycles in the voltage range 2.0–4.5 V [94]. To identify the potential of $Na_{1.4}Li_{0.6}FeP_2O_7$ in Li-ion battery, it was also tested with Li half-cell. The
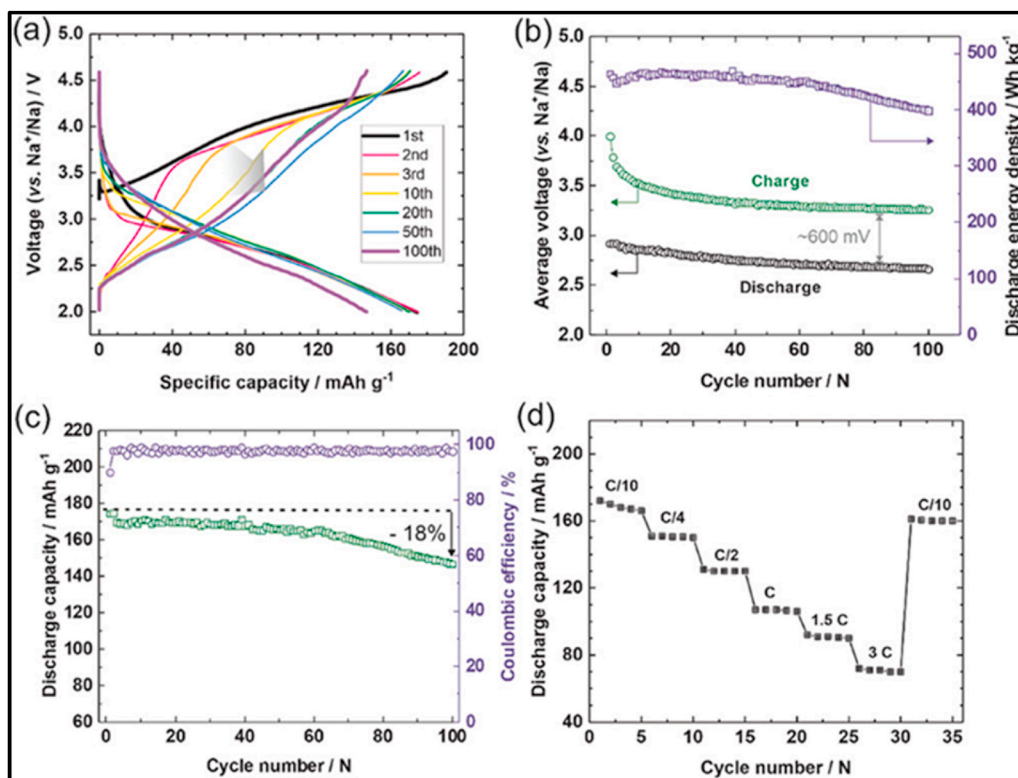
Fig. 4. a) Galvanostatic charge–discharge profiles of the $Na_{0.8}Li_{0.2}Fe_{0.2}Mn_{0.6}O_2$ cathode between 2.0 and 4.6 V at 0.1C rate; b) average charge/discharge voltage and discharge energy density (100 cycles at 0.1C rate); c) cycling data and columbic efficiency and d) rate capability (1C = 150 mA g^{-1}). Reprinted from Advanced Functional Materials, 30, L. Yang, J.M.L. Amo, Z. Shadike, S. Bak, F. Bonilla, M. Galceran, P.K. Nayak, J.R. Buchheim, X. Yang, T. Rojo, P. Adelhelm, A Co- and Ni-Free P2/O3 Biphasic Lithium Stabilized Layered Oxide for Sodium-Ion Batteries and its Cycling Behavior, 2003364, Copyright (2020), with permission from Wiley [83].

Li half-cell delivers a discharge capacity of ~85 mAhg^{-1} at 0.05C rate in the voltage window of 2.0–4.9 V with good capacity retention over the course of 50 cycles [94]. Fig. 5 shows the rate capability and cycling data for $Na_{1.4}Li_{0.6}FeP_2O_7$ cathode material. Compared to its parent material, the relatively lower performance of this material can be attributed to the amount of Li-substituted in the host structure. The incorporation of Li in the host structure of $Na_2FeP_2O_7$ causes degradation in the electrochemical performance unlike the Li incorporated Na-ion oxide cathode materials. The increased amount of Li in the structure adversely affects the performance of the material due to crystal structure destabilization. Moreover, Li-ions are not completely substituted during intercalation/deintercalation, which impedes the mobility of the Na-ions [94]. The Na in the material does not completely participate in the cycling process, which leads to lower capacity values. Furthermore, in the Li cell the Na present in the host structure acts as a pillar stabilizing the structure; hence, the displayed reversible capacity of the material is higher than that of the Na cell. On a positive note, $Na_{1.4}Li_{0.6}FeP_2O_7$

shows better thermal stability than its parent material ($Na_2FeP_2O_7$), presumably due to Li's presence in the structure. The thermogravimetric analysis (TGA) of $Na_{1.4}Li_{0.6}FeP_2O_7$ shows a comparatively lower weight loss at 550 °C. The presence of Li in higher concentrations can be a destabilizing factor in the case of Na-ion batteries. Hence, it is required to optimize Li-ion concentration in $Na_{1.4}Li_{0.6}FeP_2O_7$ for improved electrochemical performance in Na-ion batteries. In the case of the pyrophosphate materials it is necessary to have further First-principles density-functional theory (DFT) calculations to understand the complete electron transfer process occurring in the crystal structure of the material. Table 2 shows a detailed list of Li incorporated Na-ion cathode materials with their synthesis techniques and electrochemical performance.
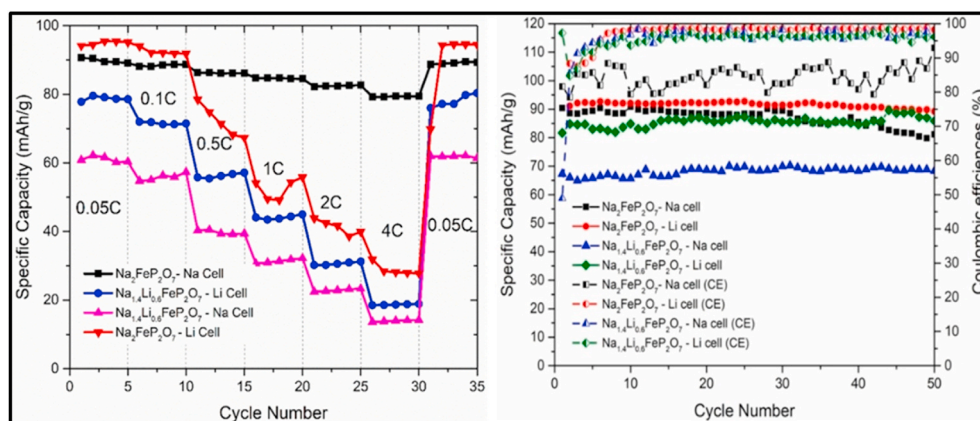

Fig. 5. Rate capability and cycling data for $Na_{1.4}Li_{0.6}FeP_2O_7$ cathode material [94].

Table 2
Li incorporated sodium based cathode materials with their synthesis techniques and electrochemical performance.

Group	Material	Synthesis technique	Initial discharge capacity (mAhg^{-1})	Capacity retention	Reference
Oxides	$Na_{0.85}Li_{0.17}Ni_{0.21}Mn_{0.64}O_2$	Ground together and fired	95–100 @ 15 mAg^{-1}	~98% after 50 cycles @ 15 mAg^{-1}	[25]
	$Na_{0.85}Li_{0.1}Ni_{0.175}Mn_{0.525}Fe_{0.2}O_2$	Co-precipitation	160 @ 0.1C	88% after 100 cycles @ 1C	[26]
	$Na_{0.80}[Li_{0.12}Ni_{0.22}Mn_{0.66}]O_2$	Co-precipitation	115 @ 0.1C	91% after 50 cycles @ 0.1C	[34]
	$Na_{0.6}Li_{0.2}Mn_{0.8}O_2$	Self-combustion reactions	~190 @ 1/15C	–	[39]
	$Na_{5/6}[Li_{1/4}Mn_{3/4}]O_2$	Solid state	150 @ 1C	–	[40]
	$Na_{0.6}Li_{0.2}Fe_{0.2}Mn_{0.6}O_2$	Self-combustion reactions	167 @ 0.2C	73% after 120 cycles at 0.2C	[46]
	$Na_{0.66}Li_{0.18}Fe_{0.12}Mn_{0.7}O_2$	Solid state	190 @ 10 mAg^{-1}	86.8% after 80 cycles @ 10 mAg^{-1}	[49]
	$Na_{0.75}Li_{0.25}Mn_{0.75}O_2$	Solid state	232 @ 0.05C	57.76% after 50 cycles @ 0.05C	[50]
	$Li_{0.2}Na_{1.0}Mn_{0.8}O_2$	Solid state	76.9 @ 50 mAg^{-1}	51.6% after 100 cycles @ 50 mAg^{-1}	[51]
	$Na_{0.6}Li_{0.07}Mn_{0.66}Co_{0.17}Ni_{0.17}O_2$	Sintering of nanoplate precursor + alkali metal carbonates	128 @ 0.5C	81% after 100 cycles @ 0.5C	[52]
	$Na_{0.8}(Li_{0.33}Mn_{0.57}Ti_{0.1})O_2$	Sol-gel	194 @ 10 mAg^{-1}	62.37% after 100 cycles @ 10 mAg^{-1}	[53]
	$Na_{0.560}[Li_{0.041}Mn_{0.642}Ni_{0.221}Ti_{0.095}]O_2$	Chemical precipitation	~130 @ 0.2C	74.2% after 100 cycles @ 0.2C	[54]
	$NaLi_{0.07}Ni_{0.26}Mn_{0.4}Co_{0.26}O_2$	Co-precipitation	110 @ 0.5C	98% after 50 cycles @ 0.5C	[65]
	$Na_{0.78}Li_{0.18}Ni_{0.25}Mn_{0.583}O_w$	Li/Na-ion exchange process	~240 @ 0.5C	86.3% after 30 cycles @ 0.5C	[67]
	$Na[Li_{0.05}(Ni_{0.25}Fe_{0.25}Mn_{0.5})_{0.95}]O_2$	Coprecipitation	180.1 @ 0.1C	89.6% after 20 cycles @ 0.2C	[77]
	$Na_{0.8}Li_{0.2}Fe_{0.2}Mn_{0.6}O_2$	Sol-gel	174 @ 0.1C	82% after 100 cycles @ 0.1C	[83]
Pyrophosphates	$Na_{1.4}Li_{0.6}FeP_2O_7$ – Na cell	Solid-state ball milling	65 @ 0.05C	–	[94]
	$Na_{1.4}Li_{0.6}FeP_2O_7$ – Li cell	Solid-state ball milling	85 @ 0.05C	–	[94]

3. Na incorporated Li-based cathode materials

3.1. Li based oxide cathode materials

3.1.1. Lithium manganese oxides (LMO's)

Oxides are one of the most common commercial cathode materials used for Li-ion batteries, and $LiCoO_2$ was the first cathode material which was commercialized in 1991 [95]. The toxic nature of cobalt (Co) compelled the use of some other transition metals as a replacement in Li-ion batteries. Out of these, Mn has considerable success for transition metal replacement in Li-ion batteries. Cathode materials like $LiMn_2O_4$ and Li_2MnO_3 are considered potential replacements due to their low synthesis cost, less toxicity, and fundamentally similar properties to $LiCoO_2$ [96–100]. However, factors like Jahn-teller lattice distortions, Mn dissolution, unstable crystal structure, and electrolyte dissolution result in poor electrochemical performance of these cathode materials [101–105]. Various techniques have been proposed to improve their electrochemical performance. Ion substitution is one of such techniques reported for improving their performance [106,107]. Na-substitution into the host structure is also another viable technique considered. Guo et al. [108] studied the effect of doping small amounts of Na into the host structure of $LiMn_2O_4$. The cathode was synthesized by the sol-gel technique keeping the weight ratio of Li: Mn as 1.05:2. The resulting phase was $Li_{1.05}Mn_2O_4$ with small concentrations of Na doped into the host structure. The synthesized pristine and sodium substituted material displays the cubic spinel structure. There are 3 major sites where the Na of the doped sample can appear, mainly the tetrahedral 8(a) site, the octahedral 16(d) site utilized by Mn ions and then the octahedral 16(c) sites, which actively play the role in Li diffusion during cycling. The reported positions where the Na occupied was the tetrahedral (8a) sites and caused the Lithium to shift to the octahedral (16d) sites and in process replacing the Mn ions. It is reported that the capacity of $Li_{1.05}Mn_2O_4$ decreases with increasing concentration of Na doped into the structure. This capacity fading can be attributed to the conversion of Mn^{3+} to Mn^{4+} due to Na's doping in the manganese spinel structure. As previously stated with increasing amounts of Na incorporated into the

crystal structure of the material, the Mn in the octahedral (16d) sites gets replaced by the Li ions arriving from the tetrahedral (8a) sites. This will result in the oxidation of Mn^{3+} ions to Mn^{4+} ion in order to electrochemically stabilize the spinel material. The Mn^{4+} ion having much small ionic radii (0.53 Å) compared to the Mn^{3+} ion (0.65 Å), results in volume shrinkage of the spinel crystal structure [109]. The shrinkage of the crystal lattice impedes diffusion of Li ions during intercalation/deintercalation, which effectively decreases the electrochemical performance of the material. The capacity of $Li_{1.05}Mn_2O_4$ relies mainly on the shifting of oxidation of Mn (Mn^{3+} to Mn^{4+}) during intercalation/deintercalation. The limited number of Mn^{3+} ions available during the charging/discharging process has an adverse impact on its electrochemical performance [108]. Furthermore, Na cannot participate in the intercalation/de-intercalation process, thereby limiting the capacity of $Li_{1.05}Mn_2O_4$. When Na is substituted in excess, the diffusion of the Li ions are adversely affected which results in increased polarity of the cathode material and decreased reversibility which limits the overall performance of the material. On the other hand, there is an increase in cycling stability due to Na doping, which acts as pillars stabilizing the crystal structure during the cycling process. Moreover, the formation of Mn^{4+} also leads to the strengthening of the Mn–O bond which improves the spinel structure stability [108]. Dong et al. [110] worked on Na-substituted $Li_{2-x}Na_xMnO_3$ (x = 0.00, 0.02, 0.05, 0.10, 0.15 and 0.20) cathode material synthesized through the solid-state reaction. Fig. 6 shows the electrochemical performance of $Li_{2-x}Na_xMnO_3$ (x = 0.00, 0.02, 0.05, 0.10, 0.15 and 0.20). Out of all the concentration of Na, $Li_{1.9}Na_{0.1}MnO_3$ cathode material shows the best overall electrochemical performance. The $Li_{1.9}Na_{0.1}MnO_3$ cathode material shows improved rate performance and cyclic stability compared to the pristine material ($Li_{1.9}Na_{0.1}MnO_3$). Fig. 6 a) shows the galvanostatic charge discharge curves of each concentration of Na added at the C/30 rate. For samples with Na >0.02, there is excess Li intercalation into octahedral sites after initial cycle. As seen from Fig. 6 b), it shows a capacity of ~181 mAhg^{-1} at 0.1C rate, with a capacity retention of 99.3% after 45 cycles. Even at an increased C-rate (0.5C), the capacity is stable at ~158 mAhg^{-1} with retention of 98.6% for 100 cycles as seen from Fig. 6 c). Whereas the
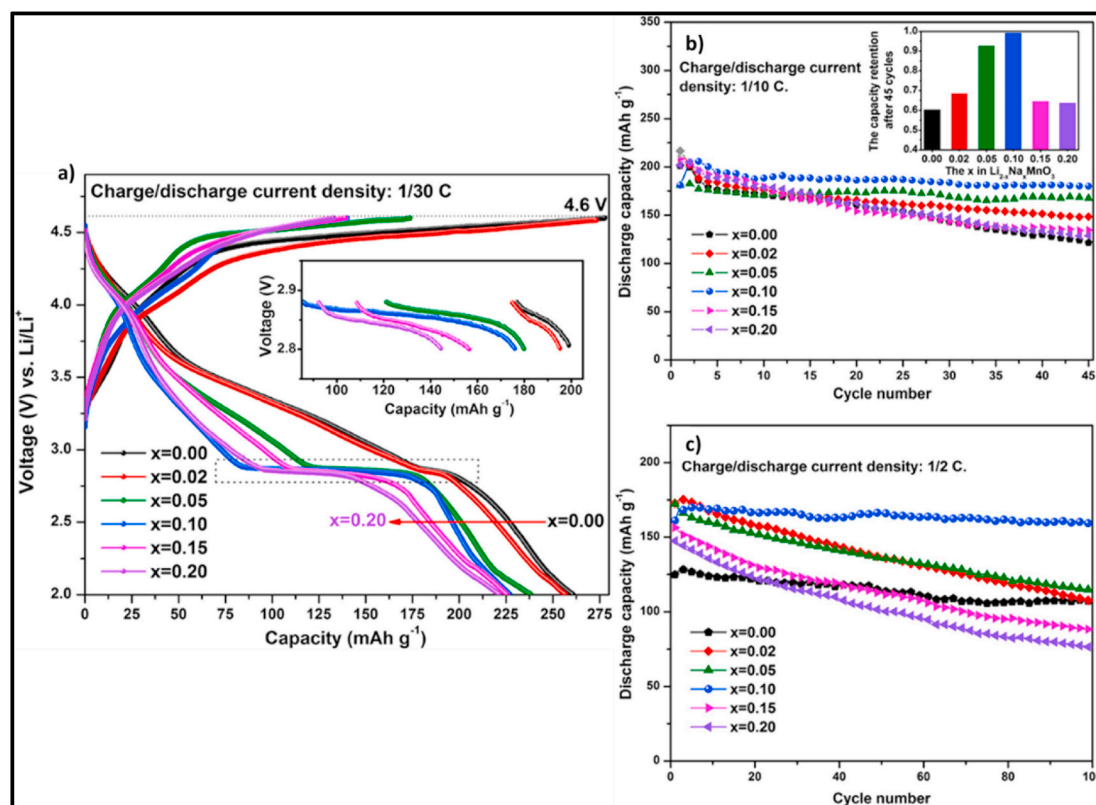
Fig. 6. Electrochemical performance of $Li_{2-x}Na_xMnO_3$ (x = 0.00, 0.02, 0.05, 0.10, 0.15 and 0.20): (a) galvanostatic charge-discharge curves at C/30 rate, (b) cycling data at C/10 rate, and (c) cycling data at C/2 rate. Reprinted from Journal of Power Sources, 243, X. Dong, Y. Xu, L. Xiong, X. Sun, Z. Zhang, Sodium substitution for partial lithium to significantly enhance the cycling stability of Li_2MnO_3 cathode material, 78–87, Copyright (2013), with permission from Elsevier [110].

pristine material shows a capacity of ~106 mAhg^{-1} with a capacity retention of 85% under identical conditions [110]. Here, the Na substitution impedes the oxygen loss and effects the spinel phase during sintering of the material, and improves electron transport at the SEI layer. Okamoto [102] reported O_2 evolution during Li-ion extraction, which causes a loss in volume and deforms the crystal structure thereby impeding cyclability of Li_2MnO_3. The incorporation of Na in the structure of LMO resulting in $Li_{1.9}Na_{0.1}MnO_3$ cathode material successfully limits oxygen evolution during the charging process by stabilizing the structure. It is however to be noted that excessive Na content in the host structure has resulted in the formation of $Na_2Mn_3O_7$ phase which destabilizes the crystal structure and unit cell shrinkages and thus negatively impacting Li-ion diffusion and cyclability [110].

3.1.2. Nickel rich layered oxides (NMC'S and NCA'S)

The NMC cathodes (cathodes with Ni, Mn, and Co in the transition layer) and NCA cathodes (cathodes with Ni, Co, and Al in the transition layer) are one of the many tried-and-tested cathode materials considered for commercial viability. Out of these, Ni-rich $LiNi_xCo_yMn_{1-x-y}O_2$ and $LiNi_xCo_yAl_{1-x-y}O_2$ (x ≥ 0.5) cathodes are mainly considered promising due to a fairly high energy density and limited synthesis cost [111,112]. Different compositions of NCA and NMC have been tested for commercial purposes and are currently used in electric vehicles like Tesla model 3 and the GM bolt [112]. Increased Ni in the structure results in the improved energy density, charge/discharge capacity, and cyclability of the cathodes [113–115]. However, an excess amount of Ni tends to inversely affect cycling performance and thermal stability, which increases safety concerns [114,116,117]. It is pertinent to mention here that Ni^{2+} has almost the same radius (0.69 Å) as the Li^+ (0.76 Å). The reduction of Ni^{3+} to Ni^{2+} causes transition metal (TM) ion migration from the TM layer to the Li layer, destabilizing the crystal structure and collapsing the interlayer space, which is the main reason for the poor

performance of these materials [112,118,119]. Various techniques have been considered to increase the interlayer spacing, and one of the most viable is Na doping. The large ionic radius of Na-ion (1.02 Å) can enlarge the Li layer spacing for better Li-ion diffusion, which improves the electrochemical performance of the Ni-rich layered oxides [120–123]. The introduction of Na atoms in the structure of NMC's is a strong driving force which limits the Li/Ni mixing and separates the Li ions from the transition metal layer [121,124]. Two Ni-rich NMCs have reported the effect of Na doping in the Ni-rich layered oxides cathodes using the same amount of Na doping (0.03 mol) [121,122]. The cathode $Li_{0.97}Na_{0.03}Ni_{0.5}Co_{0.2}Mn_{0.3}O_2$ was synthesized by the co-precipitation method, whereas the $Li_{0.97}Na_{0.03}Ni_{0.6}Co_{0.2}Mn_{0.2}O_2$ cathode was synthesized by the high-temperature solid-state technique [121,122]. The reported materials display an increase in particle with increase of Na incorporation in the materials. The increase in particle size of the materials reportedly increase the Li diffusion pathways for deintercalation/intercalation. There is an increase in capacity, especially at higher C rates, for $Li_{0.97}Na_{0.03}Ni_{0.5}Co_{0.2}Mn_{0.3}O_2$ cathode compared to the pristine material due to presence of Na [122]. The $Li_{0.97}Na_{0.03}Ni_{0.6}Co_{0.2}Mn_{0.2}O_2$ cathode also shows a similar increase in capacity compared to the pristine material, with an initial discharge capacity of 184 mAhg^{-1} at 0.1C rate and with a capacity retention of 91.67% over 100 cycles [121]. The incorporation of Na in the structure of both of these cathodes tend to increase electrochemical performance due to increased Li interface layer which is beneficial for Li-ion diffusion. Na available in the structure act as pillars preventing collapse of the Li interface layer preventing irreversible capacity loss [121,122]. The incorporation of Na in the host structure further decreases Li^+/Ni^{2+} ion exchange during charge/discharge process by preventing Ni^{2+} migration from the TM layer to Li layer [121,122]. These materials display very less Li/Ni disorder, which is beneficial for the electrochemically active redox couple Ni^{2+}/Ni^{3+} - Ni^{4+} and further prevent the alkali layer

from collapsing during the cycling process. Fig. 7 shows a schematic representing Na doping in the Li interface layer and its effect on the electrochemical performance of $Li_{1-x}Na_xNi_{0.8}Co_{0.15}Al_{0.05}O_2$ (x = 0, 0.01, 0.02, 0.05) and the inset figures show the initial charge-discharge capacity and the cycling performance of all the different concentrations of Na doping. The Na doped NCA ($Li_{0.99}Na_{0.01}Ni_{0.8}Co_{0.15}Al_{0.05}O_2$) exhibits a similar capacity to that of the pristine material; however, there is a significant improvement in cycling life. The $Li_{0.99}Na_{0.01}Ni_{0.8}Co_{0.15}Al_{0.05}O_2$ shows a capacity retention of 90.71% compared to 80.46% of the pristine material. With the increase of Na concentration in the material, there is a decrease in discharge capacities. The particular reason for this circumstance is due to electrochemical inertia of Na ions which decrease the concentration of electrochemically active Li ions in the material [120]. The Na doping in NCA has similar effects as in the case of NMC where the doping expands the Li alkali layer improving the kinetic charge transfer reaction and decreasing the activation barrier for Li ion diffusion. Furthermore, there is an additional effect of Na doping which limits the capacity fade and particle pulverization in this material by limiting H2/H3 phase transitions which would have resulted in volume changes in the crystal structure of this material [120]. The incorporation of Na in the material have decreased electrochemical polarization of the materials and also significantly improved electrochemical performance of the material.

3.1.3. Li rich layered oxides (LLO's)

Li rich layered oxides (LLOs) are seen as potential cathode material for future energy storage applications mainly due to their impressive reversible discharge capacity (>250 $mAhg^{-1}$), and good operating voltage range [125–129]. The use of LLO's are as a result of Lithium loss compensation requirement and further to limit the Li/Ni disordering occurring during cycling. However, the LLOs face many challenges such as initial irreversible capacity loss, rapid capacity and voltage decay, and poor electrochemical kinetics limiting their energy density potential [130–133]. These limitations must be overcome before cost-effective and power efficient LLOs can be successfully commercialized. Various solutions have also been presented to address the challenges such as surface modification with SiO_2, ZrO_2, Li_3PO_4, etc. [125,133,134]; controlling particle size, morphology [135,136]; and doping of transition

metals into the TM layer [137–139]. Previous theoretical studies suggested that during high voltage cycling, having low energy, causes formation of the spinel phase as the transition metal layer cations migrate towards the Li alkali layer [140,141]. However, this movement only occurs if there are three adjacent sites in the Li alkali layer which are vacant; suggesting the extreme sensitivity towards the targeted site [141,142]. Hence, incorporating other cations instead of Li can help to decrease movement of the transition layer metal ions towards the Li alkali layer for reducing voltage decay and improving electrochemical performance of the material. Like the Ni-rich NMC and NCA cathodes, Na doping was also reported in LLOs in the Li layer to increase Li layer space by the pillaring effect and prevent Li^+/Ni^{2+} disordering, leading to improved diffusion of Li-ions and thus resulting in increased cycling stability [141,143–150]. Moreover, Na doping restricts the layered-to-spinel structural transformation for LLO's as reported earlier [141].

Perhaps one of the most common LLOs is $Li_{1.2}Ni_{0.13}Mn_{0.54}Co_{0.13}O_2$, and various Na-substitution/doping, with different concentrations, have been conducted. Depending on the synthesis technique used and the concentration of Na used, varying results have been reported for $Li_{1.2}Ni_{0.13}Mn_{0.54}Co_{0.13}O_2$. All reports agree that in $Li_{1.2-x}Na_xNi_{0.13}Mn_{0.54}Co_{0.13}O_2$, Na in small concentrations ($x \leq 0.03$) improves the electrochemical performance of these cathodes due to Na protecting Li interface layer and habilitation of Li diffusion [141,143,145,146,149]. The introduction of Na into the material expands the lattice in the Li alkali layer slabs. With lattice expansion there is an increase in Li diffusion between oxygen layers during the intercalation/deintercalation process suggesting an increase in electrochemical performance of the material. The charge discharge curves and the CV curves of the pure and Na doped sample report decreased voltage and capacity decay due to presence of Na in the cathode. This is as a result of the prevention of layered to spinel transformation that usually occurs during the extraction of Li and evolution of oxygen causing voltage decays and structural instability. Increasing Na concentration in the host structure increases the material's capacity retention, which can be mainly attributed to Na's pillaring effect, which stabilizes the crystal structure. However, this is accomplished at the cost of the material's capacity as Na does not actively participate in the intercalation/deintercalation process [141,143,145,146,149]. Further beneficial effect of Na incorporation also include prevention of electrolyte degradation and development of a much more stable SEI layer improving Li diffusion [141].

The synthesis process also contributes to the performance of Na incorporated LLOs. It is reported that Na incorporation through solid-state reaction method netted a negligible increase in performance compared to other synthesis methods [146]. The particle morphology of the synthesized Na doped LLOs might also play a significant role in their observed performance. He et al. [145] synthesized 3% Na doped LLO exhibiting a cubic shaped morphology utilizing a simple polymer-pyrolysis technique. The synthesized material boasted an excellent reversible capacity of 307 $mAhg^{-1}$ at 0.1C rate with a capacity retention of 89% at 1/3C rate for 100 cycles proving its cycling stability and a reversible capacity of 139 $mAhg^{-1}$ at 8C rate which is comparable to that of the current commercial $LiCoO_2$ material [145]. The redox peaks of the synthesized Na incorporated material suggests the participation of Mn with the active redox couple of Ni and Co suggesting that the Na doping activates the Mn in the structure and thereby increase reversible capacity of the material. Furthermore, the material displays an orientation growth of the Na incorporated lattice along the direction of the alkali layer, which improves the intercalation/deintercalation process of the Li ions. The stability of this material at high current densities suggest that the structure of this material is not compromised and the Na incorporated in the structure further stabilizes it. The spherical morphology of particles obtained through different techniques such as molten salt ion-exchange method [143], surface doping with NaCl flux molten-slat method [151], hydrothermal method [141], and
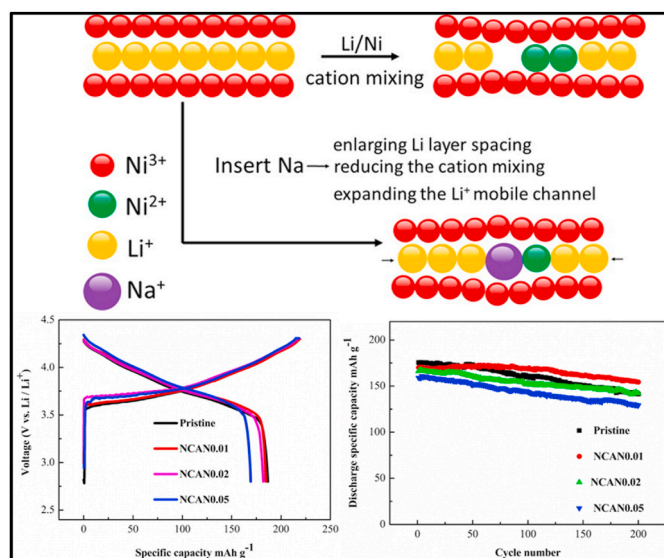

Fig. 7. Schematic diagram of Li interface layer and electrochemical performance of $Li_{1-x}Na_xNi_{0.8}Co_{0.15}Al_{0.05}O_2$ (x = 0, 0.01, 0.02, 0.05). Reprinted (adapted) with permission from Journal of Physical Chemistry C, 120, H. Xie, K. Du, G. Hu, Z. Peng, Y. Cao, The Role of Sodium in $LiNi_{0.8}Co_{0.15}Al_{0.05}O_2$ Cathode Material and Its Electrochemical Behaviors, 3235–3241. Copyright (2016) American Chemical Society [120].

co-precipitation technique [144] has also been reported. All the reports indicate a significant increase in capacity and capacity retention with Na incorporation in the host structure [141,143,144,151]. The molten salt ion-exchange method material study reported that increase in Na concentration resulted in formation of a secondary phase and Na deintercalation during first charge. But, with the rest of the cycles, the Na remains in the crystal structure without actively participating in the cycling process [143]. There have been some reports elucidating the effect of Na doping on many other LLOs with different Li and TM concentrations like $Li_{1.17}Ni_{0.10}Co_{0.10}Mn_{0.63}O_2$, $Li_{1.167}Ni_{0.18}Mn_{0.548}$-$Co_{0.105}O_2$, and $Li_{1.1-x}Na_x[Ni_{0.2}Co_{0.3}Mn_{0.4}]O_2$ [147,148,150]. All these materials have reported enhancements in electrochemical performance due to Na incorporation.

3.2. Phosphate cathode materials

The olivine-type $LiMPO_4$ (M = Metal Substituents such as; Na, and high-valent metal substituents such as V, Mn) shows promising results with intrinsically high safety brought about by the P–O bond, environmentally friendly nature, and low cost [152–154]. Some profound examples of pristine olivine-type materials are $LiFePO_4$ and $LiMnPO_4$. The olivine type cathode materials have theoretical capacities of ~ 170 $mAhg^{-1}$, which is comparatively lower than the silicate family of cathode materials. The olivine type cathode materials also suffer from poor electronic and ionic conductivity and a slow Li-ion diffusion [152–155]. Therefore, the incorporation of metal and/or high-valent metal substituents has been investigated in multiple studies by doping and co-doping to further improve olivine type $LiMPO_4$ performance. The synthesis route of $LiMPO_4$ is generally solid-state or sol-gel reaction [152–155]. Specifically, the effects of Na-doping and Na/V co-doping in $LiFePO_4$ have been studied by Yin et al. [152] and Yang et al. [155], respectively, and their findings complement each other. The Na-doped $Li_{1-x}Na_xFePO_4/C$ system studied by Yin et al. [152] reports that doping in $0 \leq x \leq 0.05$ worth of Na that a ratio of 0.03 was optimal. Fig. 8 shows the electrochemical performance of $Li_{1-x}Na_xFePO_4/C$ ($\leq$ x $\leq$ 0.05). It is reported that the smaller ratios of Na would provide a negligent change in the lattice size, and the system does not experience an improved Li-ion diffusion pathway. However, the upper limit of the ratio at 0.05 Na produced counter-productive results. At the perfect ratio of $Na_{0.03}$, it was reported that there exists the widest Li-ion diffusion channel and shortest diffusion pathway – hence better facilitating the intercalation/de-intercalation process [152,155]. As seen in Fig. 8 a) the $Na_{0.03}$ doping of the $Li_{1-x}Na_xFePO_4/C$ samples reached the highest initial special discharge capacity of 158 $mAhg^{-1}$ amongst other Na_x doping amounts – specifically as compared to pristine $LiFePO_4/C$ with

initial specific discharge capacity 151 $mAhg^{-1}$ at 0.1C rate, which is indicative of better conductivity brought about by Na-doping. Moreover, Fig. 8 b) highlights that $Na_{0.03}$ also performed better in capacity retention studies, up to 50 cycles, whilst maintaining the advantage a of greater specific capacity. The cyclic voltammetry study of $Li_{0.97}Na_{0.03}$-$FePO_4/C$ exhibited much sharper and more narrow separation of current peaks, which suggests better reversible electrode reactions. At the same time electrochemical impedance spectroscopy (EIS) studies showed less electrical resistance [152]. Specifically, as seen in Fig. 8 Ouyang et al. [156] reported that high-valent metal doping blocks the one-dimensional diffusion channel of Li-ions in olivine-type $LiMPO_4$ systems. Studies on co-doping via Na/V substituents revealed that this blocking effect was nullified [156,157]. As demonstrated by Yang et al. [155] the $Li_{1-x}Na_xFe_{1-x}V_xPO4/C$ had a similar increased specific discharge to 156.5 $mAhg^{-1}$ as compared to pristine with the greatest effect at $Na_{0.03}$-$V_{0.03}$ ratios. Cycling profile of $Li_{0.97}Na_{0.03}$-$Fe_{0.97}V_{0.03}PO_4/C$ also showed less capacity fading, which could correspond to better structural stability. Studies into a different variant of the material, $LiMnPO_4$ and its constituents have also been investigated – showing the same results as seen in the previous $Li_{1-x}Na_xFe_{1-x}V_xPO_4/C$ [155]. El Khalfaouy et al. [28] reported that even in $Li_{0.97}Na_{0.03}Mn$-PO_4/C, synthesized by solution combustion method, had an initial discharge capacity of 136.7 $mAhg^{-1}$ at 0.05C rate with coulombic efficiency of 93.8%. The both aspects (discharge capacity and coulombic efficiency) are higher than its pristine counterpart exhibiting initial discharge capacity 126.9 $mAhg^{-1}$ and 82.3% coulombic efficiency. Furthermore, higher ratios of 0.3 Na in the olivine-type $LiMPO_4$ was studied by Zhang et al. [158], when compared to pristine samples, the modified cathode material has demonstrated much higher initial discharge capacity (152 $mAhg^{-1}$ at 0.05C rate) and better capacity retention. In summary, it is established that Na-incorporation not only improves the Li-ion diffusion paths by increasing the lattice volume, but it also reduces the polarization brought about by the Jahn-Teller effect for high-valent substituents, specifically manganese based $LiMPO_4$ as Na directly affects the M–M distance when substituting a Li-ion [28,159,160].

In addition to Na-substitution, coating techniques such as that of carbon and more exclusively reduced graphene oxide (rGO) have exhibited synergistic effect by restricting the growth of $LiMPO_4$ crystals and providing a conductive network surrounding the $LiMPO_4$ material enabling to achieve initial discharge capacities of more than 100 $mAhg^{-1}$ at 10C [159,161,162].

The effect of Na-incorporation on lithium transition metal phosphates, represented as $Li_{1-x}M_y(PO_4)_z$, has also been investigated to improve their poor intrinsic conductivity, cyclability, and rate
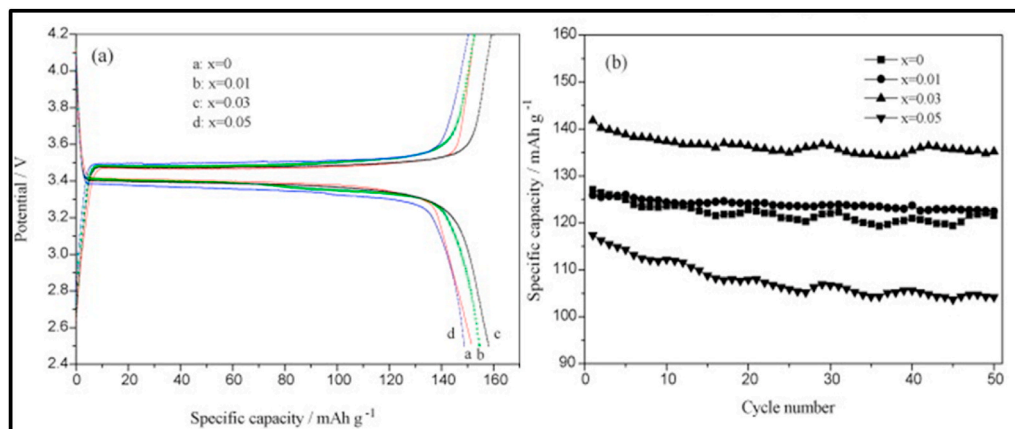

Fig. 8. (a) Galvanostatic charge and discharge curves of $Li_{1-x}Na_xFePO_4/C$ ($0 \leq x \leq 0.05$) electrodes at 0.1 C and (b) cycle performance of electrodes at 1 C. Reprinted from Journal of Power Sources, 195, X. Yin, K. Huang, S. Liu, H. Wang, H. Wang, Preparation and characterization of Na-doped $LiFePO_4/C$ composites as cathode materials for lithium-ion batteries, 4308–4312, Copyright (2010), with permission from Elsevier [152].

capabilities [163–166]. Although there are pre-existing techniques like carbon coating to improve the above stated three intrinsic imperfections, Na-doping at small amounts has less likelihood to diminish the energy density of the material [163]. $Li_{3-x}Na_xV_2(PO_4)_3$/C is a prime example that has been synthesized more commonly by sol-gel reaction instead of by rheologic phase reaction [163,166]. It is reported by Wang et al. [163] that at $N_{0.03}$ ratio is the terminal point where there is a maximum improvement in the intrinsic properties of the material. This is specifically prevalent in the cyclability performance of the $Li_{3-x}Na_xV_2(PO_4)_3$/C where after 30 cycles at 0.1C rate $Li_{2.97}Na_{0.03}V_2(PO_4)_3$/C experienced only 1.5% capacity loss, while pristine $Li_3V_2(PO_4)_3$ experienced 18.8% loss [163]. The improved capacity retention is basically originated from the Pillar effect of Na preventing structural collapse [163,167]. On the other hand, a comparison of initial specific discharge capacities of both materials (pristine and doped) indicates a minimal increase of capacity [163,166]. This effect was attributed to multiple studies where Na-doping does not block the diffusion pathways for Li-ions, consequently not affecting the materials' capacities [163,166]. Measurements of the electronic conductivity by Kuang et al. [166] showed an increase in the electronic conductivity at $Na_{0.03}$ of 6.74×10^{-3} Scm^{-1} as compared to the pristine $Li_3V_2(PO_4)_3$ of 2.16×10^{-4} Scm^{-1}. This improvement was attributed to the expansion of cell volume and narrowing of bandgap as the V positions get distorted when Na is substituted into the system. Interestingly, there exists NASICON hybrid-phased $Li_2NaV_2(PO_4)_3$ possessing characteristics of monoclinic $Li_3V_2(PO_4)_3$ and rhombohedral $Na_3V_2(PO_4)_3$ synthesized due to having better reversible capacity compared to single-phased $Li_2NaV_2(PO_4)_3$ as well as having better intrinsic characteristics i.e. diffusion rates and electrochemical behaviors [168,169]. Based on results from Li et al. [168], the hybrid-phased $Li_2NaV_2(PO_4)_3$ has shown increased chemical diffusion coefficients as compared to the single components (pristine) in all anodic and cathodic peaks, highlighting the enhancement of electrical conductivity due to hybrid structure.

3.3. Silicate cathode materials

Polyanionic-based systems notably silicates are garnering much attention in the past few years as compared to their phosphate counterpart. The silicates materials project higher theoretical capacities due to the increased reversible cyclability of the lithium ions [170]. Notable characteristics of silicate polyanionic based systems attribute to the Si–O bond, which allows for high safety and thermal stability aside from the minimal negative environmental impact [27]. Specifically, silicate systems such as Li_2XSiO_4 (X = Co or Mn) are worked out well due to their high theoretical capacity (~ 325–330 mAhg^{-1}). Despite possessing advantageous characteristics, Li_2XSiO_4 experiences poor electrical and ionic conductivities; in particular, the sluggish lithium-ion diffusion mobility accounts for the material's impracticality for energy storage applications. Although carbon coating techniques have been applied to correct these imperfections [27,170,171]. Some studies are focused on using magnesium (Mg) or iron (Fe) substitution to improve conductivity and cyclability. These techniques have demonstrated some positive impact but remain under expectations, thus pointing in Na-substitution direction. Many members of the Li_2XSiO_4 family have been synthesized by either sol-gel or hydrothermal method. Studies focused on Na-substitution in Li_2CoSiO_4 have shown improved electrical conductivity due to the expansion of unit cell parameters in as reported by Wu et al. [170]. This feature is particularly important for Li_2CoSiO_4 whose crystalline structure consists of corrugated layers - therefore, the structural expansion of said layers positively affects the pathways for diffusion of Li-ions, thereby increasing the conductivity. Furthermore, in the same study, through band structure measurements, it is noticed that $Li_{1.5}Na_{0.5}CoSiO_4$ exhibits a slightly reduced gap ($\sim 9.8\%$) between the valence band maximum and conduction band minimum as compared to pristine Li_2CoSiO_4, which leads to better electrical conductivity. Succeeding studies of Li_2CoSiO_4 by Zhang et al. [27] corroborate the

improved performance of the said system employing Na-substitution. It is reported that Na substitution in Li_2CoSiO_4 also decreases the activation barriers and increases the hopping distance within the diffusion paths. Such effects assist the ease of migration for Li-ions [27,170]. Distinctively, the amount of Na added into the system will create different effects on the silicate system. A study of Wang et al. [171] on Li_2MnSiO_4, reports that $Li_{1.9}Na_{0.1}MnSiO_4$ outperforms than $Li_{1.8}Na_{0.2}MnSiO_4$. $Li_{1.9}Na_{0.1}MnSiO_4$ exhibits the highest capacity in the tested current densities and has a greater initial discharge capacity of ~ 175 mAhg^{-1} compared to $Li_{1.8}Na_{0.2}MnSiO_4$ (~ 143 mAhg^{-1}). Both modified materials outperform when compared to the pristine Li_2MnSiO_4 because of the Na-ions' ability to suppress the growth of Li_2MnSiO_4 crystals and improve the ionic/electronic transfer interface, which then enhances electrochemical reactions [171]. However, through Rietveld refinement, the study further reports that there is a decrease in the particle size due to the incorporation and further there is no significant improvement observed in the cyclic stability of the material mainly due to the poor surface electrochemical activity [171]. Overall, the use of Na allows for better conductivity through increased lattice parameters and finer particle size. It should be noted that Na-substitution can be used in conjunction with carbon coating for a further decrease in particle size and better discharge capacity [171]. The use of carbon coating will improve electronic conductivity of the material and limit particle size growth, which can facilitate faster Li diffusion channels for cycling. Furthermore, the carbon coating will reduce the electrochemical polarization of the material which is beneficial for reversible Li intercalation/deintercalation from the structure. A brief report on different Na incorporated cathode materials, their synthesis method, and electrochemical performance is given in Table 3.

4. Summary and outlook

Various advancements in the field of Li/Na incorporated cathode materials have been observed in the past decades. This review precisely and briefly reports the synthesis and electrochemical performance of various families of Li/Na incorporated cathode materials developed for Na/Li-ion batteries. Mainly, the effect of Li incorporation in Na-based cathode materials and the impact of Na addition in Li-based cathode materials have been reviewed. The incorporation of Li in Na based cathode materials leads to improved electrochemical performance, which is beneficial for developing high energy density Na-ion batteries. The Li in the Na-ion battery cathode material prevents the destructive phase transformations at high voltages by occupying the alkali layer from the transition metal layer during deintercalation and returns back to the transition metal layer during intercalation. In the case of the oxide based materials for the Na-ion battery materials, it also limits the Jahn teller distortions occurring. In the Na-ion battery cathode materials, the presence of Li is known to have a dual stabilization effect of preventing Jahn-teller distortions and preventing transition metal ion loss by securing the cathode-electrolyte interphase. The biphasic oxide cathodes provide a new avenue towards cathodes with properties of both P2 phase and O3 phase, which improves electrochemical performance and stability by facilitating smooth Na diffusion. The Li incorporated Na-ion pyrophosphate cathode materials however has not shown improvement electrochemically while showing a slight improvement in thermal stability. The pyrophosphate family of materials however have a potential for application in batteries due to their excellent thermal and crystal structure stability, and with further optimization to the concentration of Li incorporation and study using first principle DFT calculations. In terms of electrochemical performance of all the Li incorporated Na-ion battery cathode materials, the O3 type - $Na_{0.78}Li_{0.18}Ni_{0.25}Mn_{0.583}O_w$ cathode material reported by the Liu group through the Li/Na-ion exchange process exhibited the best electrochemical performance [67]. It delivered a capacity of 240 mAhg^{-1} at 0.5C rate and cycling stability for 30 cycles with a capacity retention of 190 mAhg^{-1}. The energy density delivered by this material (675 WhKg^{-1}) was greater than the energy

Table 3
Na incorporated cathode materials with their synthesis techniques and electrochemical performance.

Group	Material	Synthesis technique	Initial discharge capacity (mAhg^{-1})	Capacity retention	Reference
Oxides	$Li_{1.05}Mn_2O_4 - 3\%$ Na	Sol-gel	107.9 @ 0.5C	97% after 25 cycles @ 0.5C	[108]
	$Li_{1.90}Na_{0.10}MnO_3$	Solid-State	181 @ 0.1C	99.3% after 45 cycles @ 0.1C	[110]
	$Li_{0.99}Na_{0.01}Ni_{0.8}Co_{0.15}Al_{0.05}O_2$	Co-precipitation and solid-state calcination	184.6 @ 0.1C	90.71% after 200 cycles @ 1 C	[120]
	$Li_{0.97}Na_{0.03}Ni_{0.6}Co_{0.2}Mn_{0.2}O_2$	High-temperature solid method	184 @ 0.1C	91.67% after 100 cycle @ 1C	[121]
	$Li_{0.97}Na_{0.03}Ni_{0.5}Co_{0.2}Mn_{0.3}O_2$	Hydroxide co-precipitation	228.43 @ 0.2C	–	[122]
	$Li_{0.95}Na_{0.05}Ni_{1/3}Co_{1/3}Mn_{1/3}O_2$	Co-precipitation	250.5 @ 0.1C	99.02% after 110 cycles @ different C rates	[123]
	$Li_{1.15}Na_{0.05}[Ni_{0.13}Co_{0.13}Mn_{0.54}]O_2$	Hydrothermal method	~230 @ 0.1C	85.5% after 100 Cycles @ 1C	[141]
	$Li_{1.2}Mn_{0.54}Ni_{0.13}Co_{0.13}O_2 - 0.25\%$ Na doped	Molten salt ion exchange	274 @ 0.1C	92.23% after 100 cycles @ 1C	[143]
	$Li_{1.166}Na_{0.032}Mn_{0.532}Ni_{0.132}Co_{0.136}O_2$	Co-precipitation	279 @ 0.1C	–	[144]
	$Li_{1.17}Na_{0.03}[Co_{0.13}Ni_{0.13}Mn_{0.54}]O_2$	Polymer-pyrolysis	307 @ 0.1C	89% after 100 cycles at 1/3C	[145]
	$Li_{1.18}Na_{0.02}Ni_{0.13}Co_{0.13}Mn_{0.54}O_2$	Solid-State	288 @ 0.1C	77.8% after 50 cycles @ 0.5C	[146]
	$Li_{1.05}Na_{0.05}[Ni_{0.2}Co_{0.3}Mn_{0.4}]O_2$	Sol-gel	195 @ 0.25C	92% after 50 cycles @ 0.25C	[147]
	$Li_{1.117}Na_{0.05}Ni_{0.18}Mn_{0.548}Co_{0.105}O_2$	Spray pyrolysis	208 @ 1C	92% after 50 cycles @ 0.5C	[148]
	$Li_{1.1}Na_{0.1}Mn_{0.54}Co_{0.13}Ni_{0.13}O_2$	Confinement method	242 @ 0.1C	88.8% after 50 cycles @ 0.1C	[149]
	$Li_{1.11}Na_{0.06}Ni_{0.01}Co_{0.01}Mn_{0.63}O_2$	Carbonate co-precipitation for precursor, Solid-state	194.9 @ 1C	94.9% after 50 cycles @0.5C	[150]
	$0.5Li_2MnO_3.0.5LiNi_{1/3}Co_{1/3}Mn_{1/3}O_2 - 0.4\%$ Na doped on surface	Co-precipitation for precursor, NaCl flux via molten salt method	286 @ 0.1C	87.9% after 100 cycles @ 0.2C	[151]
	$Li_{0.99}Na_{0.01}Mn_2O_4$	Solid-State	125.1 @ 0.5C	92.3% after 100 cycles @ 0.5C	[172]
	$Li_{0.95}Na_{0.05}Ni_{0.5}Mn_{1.5}O_4$	Co-precipitation for precursor, High-temperature pyrolysis.	125 @ 1C	92.96% after 100 cycles @ 1C	[173]
Phosphates	$Li_{0.97}Na_{0.03}MnPO_4/C$	Modified solution combustion	136.7 @ 0.05C	90.2% after 50 cycles @ 0.1C	[28]
	$Li_{0.97}Na_{0.03}FePO_4/C$	In-situ polymerization restriction–carbon thermal reduction	158 @ 0.1C	~93% after 50 cycles @ 0.1C	[152]
	$Li_{0.97}Na_{0.03}Fe_{0.97}V_{0.03}PO_4/C$	Solid-State	156.5 @ 0.1C	97.6% after 50 cycles @ 0.1C	[155]
	$Li_{0.9}Na_{0.1}MnPO_4/C$	Simple Hydrothermal	152 @ 0.05C	93.8% after 200 cycles @ 0.1C	[158]
	$Li_{2.95}Na_{0.05}V_2(PO_4)_3/C$	Rheologic phase reaction	131.1 @ 0.1C	94.3% after 30 cycles @ 0.1C	[163]
	$Li_{2.97}Na_{0.03}V_2(PO_4)_3/C$	Solid-state	118.9 @ 2C	88% after 80 cycles	[166]
	$Li_{0.99}Na_{0.01}VPO_4F$	Soft chemical rout with mechanical activation assist	136 @ 0.5C	95.5% after 50 cycles @ 0.5C	[174]
Silicates	$Li_{1.9}Na_{0.1}MnSiO_4/C$	Sol-Gel	175 @ 0.1C	27% after 40 Cycles @ 0.1C	[171]

densities of the commercial cathode materials LiFePO$_4$ and LiCoO$_2$ (560 WhKg^{-1}) utilized in Li-ion batteries [67,175–177]. Moreover, the cobalt-free cathode materials considerably decreases the raw material cost for the reagents required to prepare the material. Hence, the high energy density, cyclic stability, and lower raw material cost of this material make it one of the best electrochemically performing materials for Na-ion and Li-ion batteries. For the future of Na-ion cathode materials, it is necessary to focus on the Li incorporated materials as it improves the performance of these cathode materials by a large margin.

The Na incorporation in Li-based cathodes results in improved cyclic stability and capacity retention, which is extremely beneficial for long-lasting batteries. Na acts as a pillar in the Li-ion cathode preventing Li$^+$/Ni^{2+} disordering, improving Li-ion diffusion, and preventing Ni^{2+} ion migration towards the Li layer. This pillar effect of the Na improves the cycling stability of the Li-ion cathode materials resulting in longer lasting batteries. However, excessive addition of Na in the cathode material decreases the overall capacity performance of the materials as it limits the active number of Li ions in the crystal structure used for cycling. In the case of the Na incorporated Li-ion phosphate and silicate

cathode materials, the Na improves the diffusion pathways of the Li-ion by slightly influencing the crystal lattice of the sample. It also decreases the activation barriers of the materials and increases hopping distance in the diffusion pathways thereby increasing migration of Li-ion during cycling. For the Na incorporated Li-ion battery cathode materials, the lithium-rich layered oxides (LLO's) outperforms all the normal oxide materials in terms of electrochemical performance. In the LLO's the Li$_{1.17}$Na$_{0.03}$[Co$_{0.13}$Ni$_{0.13}$Mn$_{0.54}$]O$_2$ cathode material prepared by He et al. [145] utilizing the polymer-pyrolysis method delivers a reversible discharge capacity of 307 mAhg^{-1} at 0.1C rate and cycling stability for 100 cycles with capacity retention of 89% at 1/3C rate. This is mainly attributed to the cubic particle morphology displayed by the material when doped with Na, improving the crystal growth along the layers [145]. Within the LLO's the cubic particle morphology Li$_{1.17}$Na$_{0.03}$[Co$_{0.13}$Ni$_{0.13}$Mn$_{0.54}$]O$_2$ cathode material has an overall capacity increase compared to the other LLO materials. Therefore, it is important to note that particle morphology plays an important role in improving the electrochemical performance of the material. In the case of the Na incorporated Li-ion cathode materials, it is necessary to identify the

limiting concentration of Na required before the capacity performance of materials are decreasing. Hence, the trade-off between capacity and cycling stability need to be analyzed to develop materials having the best energy and power density. Owing to their promising electrochemical performance (high energy density, cyclic stability, and improved capacity retention), the reported cathode materials may be promising for future battery applications.

With the increasing number of reports on Na/Li incorporated cathode materials for Li/Na-ion batteries, various other studies have emerged that incorporate other alkali metals such as potassium (K), in the cathode material [178–185]. However, due to the similar properties exhibited by the Na/Li incorporated cathode materials, the K incorporated Na/Li-ion batteries also tend to experience similar electrochemical behavior as the former. The K ion acts as pillar ion's due to their large ionic radii which facilitate easy diffusion of Na/Li ions for their respective batteries and prevents the collapse of the structure after successive cycles of Na/Li diffusion [178–180,183]. These types of cathode material that incorporate K ions which support the structural framework of the material have been recently named "pillar beam" structures [184]. Compared to the Na ions incorporated in a Li-ion cathode material, which might migrate toward the electrolyte during high voltage electrochemical tests, the K ions rarely tend to participate in ion diffusion during electrochemical tests [183]. The K ions are usually localized in the structure and this causes them to have migration barriers that require very high activation energy requirements to migrate to the adjacent sites. Hence, the K ions tend to remain inactive in Na/Li cathode material structures [184]. Most studies reported improved reversible capacity and cycling stability which resulted in higher energy density cathode materials suggesting the viability of this K ion incorporation into the cathode material of Li/Na-ion batteries. Hence, the strategy of alkali metal incorporation into cathode material structure for Na/Li-ion batteries may be considered a potential solution for future energy storage applications.

The studies on Li/Na incorporated cathode materials for Na/Li-ion batteries have culminated in the improvement of reversible capacity, cycling stability, energy density, and overall electrochemical performance of various mainstream cathode materials. However, for this field of study, optimization and improvement of various parameters are required to facilitate their commercialization. Optimization of the doping/substitution concentration of the Li/Na is a major challenge that needs to be addressed for better electrochemical performance in batteries. Identifying accurate concentration of dopant/substituent will enable extracting the maximum potential from the material without negatively influencing the performance of the material. Particle morphology is another factor that plays an important role in electrochemical performance. As seen from the LLO material with cubic particle morphology, it delivered increased capacity compared to the materials with less well-defined particle morphology. Further suggestions include co-doping of the alkali metal layer with K ions, or transition metal layer with Ti, Fe, Nb, F, etc. which can improve structural stability, cyclability, and electrochemical performance of the materials. In terms of further improvements that can improve the performance of these Li/Na incorporated materials, various techniques can be employed such as reduction of particle size, which can benefit with faster Li/Na diffusion pathways, and ceramic coatings on the particles, which can protect the particles from unwanted side reaction when in contact with the electrolyte. However, the cost outlook on the utilization of these techniques seems unrealistic during commercialization process. In terms of commercialization plans, the viability of the synthesis method needs to be analyzed. More cost-efficient processes are required before the Na/Li incorporated cathode materials can achieve commercialization. The use of Co-free cathodes should also be encouraged for future studies as it can considerably cut raw material costs in batteries. Depending on the synthesis procedure of these cathode materials, low cost batteries are viable for commercialization with improved electrochemical performance and cyclability. Developing Li/Na incorporated cathode

materials can be cost efficient owing to the limited Li reserves and if the incorporated materials show better cyclability and capacity, it is a step towards more cost efficient batteries. Addressing the above-stated issues can facilitate to development of cathode materials with cheaper synthesis costs demonstrating improved electrochemical performance. A focused review in this important area as presented herein may facilitate to understand the science and governing mechanism of existing Li/Na incorporated cathode materials leading to more innovations and developments to fabricate high-performance future batteries for energy storage applications.

CRediT authorship contribution statement

Declaration of competing interest

The authors declare that they have no known competing financial interests or personal relationships that could have appeared to influence the work reported in this paper.

Acknowledgments

References

[1] A.V. Shaikh, S.G. Sayyed, S. Naeem, R.S. Mane, Electrodeposition of n-CdSe/p-Cu2Se heterojunction solar cells, Eng. Sci. (2020), https://doi.org/10.30919/es8d1124.

[2] Q.-Y. Li, Q. Hao, T. Zhu, M. Zebarjadi, M. Zebarjadi, Nanostructured and heterostructured 2D materials for thermoelectrics, Eng. Sci. (2020), https://doi.org/10.30919/es8d1136.

[3] G.K. Rahane, S.B. Jathar, S.R. Rondiya, Y.A. Jadhav, S.V. Barma, A. Rokade, R.W. Cross, M.P. Nasane, V. Jadkar, N.Y. Dzade, S.R. Jadkar, Photoelectrochemical investigation on the cadmium sulfide (CdS) thin films prepared using spin coating technique, ES Mater. Manuf. (2020), https://doi.org/10.30919/esmm5f1041.

[4] D. Pan, F. Su, H. Liu, C. Liu, A. Umar, L. Castañeda, H. Algadi, C. Wang, Z. Guo, Research progress on catalytic pyrolysis and reuse of waste plastics and petroleum sludge, ES Mater. Manuf. (2021), https://doi.org/10.30919/esmm5f415.

[5] S.D. Satpute, J.S. Jagtap, P.K. Bhujbal, S.M. Sonar, P.K. Baviskar, S.R. Jadker, H.M. Pathan, Mercurochrome Sensitized ZnO/In2O3 Photoanode for Dye-Sensitized Solar Cell, ES Energy Environ. (2020), https://doi.org/10.30919/esee8c720.

[6] D. Li, J. Sun, R. Ma, J. Wei, High-efficient and Low-Cost H2 Production by Solar-Driven Photo-Thermo-Reforming of Methanol with CuO Catalyst, ES Energy Environ. (2020), https://doi.org/10.30919/esee8c722.

[7] Y. Zhou, S. Wu, Y. Ma, H. Zhang, X. Zeng, F. Wu, F. Liu, J.E. Ryu, Z. Guo, Recent Advances in Organic/Composite Phase Change Materials for Energy Storage, ES Energy Environ. (2020), https://doi.org/10.30919/esee8c150.

[8] J. Wang, Y. Liu, Z. Fan, W. Wang, B. Wang, Z. Guo, Ink-based 3D printing technologies for graphene-based materials: a review, Adv. Compos. Hybrid Mater. 2 (2019) 1–33, https://doi.org/10.1007/s42114-018-0067-9.

[9] C. Hou, J. Hou, H. Zhang, Y. Ma, X. He, W. Geng, Q. Zhang, Facile synthesis of LiMn0.75Fe0.25PO4/C nanocomposite cathode materials of lithium-ion batteries through microwave sintering, Eng. Sci. (2020), https://doi.org/10.30919/es5e1006.

[10] G. Li, C. Dang, Y. Hou, F. Dang, Y. Fan, Z. Guo, Experimental and theoretical characteristic of single atom Co-N-C catalyst for Li-O2 batteries, Eng. Sci. (2020), https://doi.org/10.30919/es8d1005.

[11] M.T. Dizaji, W. Li, Higher voltage redox flow batteries with hybrid acid and base electrolytes, Eng. Sci. (2020), https://doi.org/10.30919/es8d1118.

[12] C. Hou, B. Wang, V. Murugadoss, S. Vupputuri, Y. Chao, Z. Guo, C. Wang, W. Du, Recent advances in Co3O4 as anode materials for high-performance lithium-ion batteries, Eng. Sci. (2020), https://doi.org/10.30919/es8d1128.

[13] H. Tong, Q. Zhou, B. Zhang, X. Wang, Y. Yao, Z. Ding, H. Chen, J. Zheng, W. Yu, A novel core-shell structured nickel-rich layered cathode material for high-energy lithium-ion batteries, Eng. Sci. (2020), https://doi.org/10.30919/es8d502.

[14] Y. Li, X. Wang, Z. Wang, L. Chen, Facile Synthesis of SnO Nanorods for Na-Ion Batteries, ES Energy Environ. (2019), https://doi.org/10.30919/esee8c198.

[15] M. Idrees, L. Liu, S. Batool, H. Luo, J. Liang, B. Xu, S. Wang, J. Kong, Cobalt-doping enhancing electrochemical performance of silicon/carbon nanocomposite as highly efficient anode materials in lithium-ion batteries, Eng. Sci. (2019), https://doi.org/10.30919/es8d798.

[16] C. Liu, R. Massé, X. Nan, G. Cao, A promising cathode for Li-ion batteries: Li3V2 (PO4)3, Energy Storage Mater. 4 (2016) 15–58, https://doi.org/10.1016/j.ensm.2016.02.002.

[17] W. Chen, J. Liang, Z. Yang, G. Li, A review of lithium-ion battery for electric vehicle applications and beyond, in: Energy Procedia, Elsevier Ltd, 2019, pp. 4363–4368, https://doi.org/10.1016/j.egypro.2019.01.783.

[18] N. Nitta, F. Wu, J.T. Lee, G. Yushin, Li-ion battery materials: present and future, Mater. Today 18 (2015) 252–264, https://doi.org/10.1016/j.mattod.2014.10.040.

[19] H. Vikström, S. Davidsson, M. Höök, Lithium availability and future production outlooks, Appl. Energy 110 (2013) 252–266, https://doi.org/10.1016/j.apenergy.2013.04.005.

[20] N. Yabuuchi, K. Kubota, M. Dahbi, S. Komaba, Research development on sodium-ion batteries, Chem. Rev. 114 (2014) 11636–11682, https://doi.org/10.1021/cr500192f.

[21] J.Y. Hwang, S.T. Myung, Y.K. Sun, Sodium-ion batteries: present and future, Chem. Soc. Rev. 46 (2017) 3529–3614, https://doi.org/10.1039/c6cs00776g.

[22] V. Palomares, P. Serras, I. Villaluenga, K.B. Hueso, J. Carretero-González, T. Rojo, Na-ion batteries, recent advances and present challenges to become low cost energy storage systems, Energy Environ. Sci. 5 (2012) 5884–5901, https://doi.org/10.1039/c2ee02781j.

[23] K.M. Abraham, How comparable are sodium-ion batteries to lithium-ion counterparts? ACS Energy Lett. 5 (2020) 3544–3547, https://doi.org/10.1021/acsenergylett.0c02181.

[24] B.L. Ellis, L.F. Nazar, Sodium and sodium-ion energy storage batteries, Curr. Opin. Solid State Mater. Sci. 16 (2012) 168–177, https://doi.org/10.1016/j.cossms.2012.04.002.

[25] D. Kim, S.H. Kang, M. Slater, S. Rood, J.T. Vaughey, N. Karan, M. Balasubramanian, C.S. Johnson, Enabling sodium batteries using lithium-substituted sodium layered transition metal oxide cathodes, Adv. Energy Mater. 1 (2011) 333–336, https://doi.org/10.1002/aenm.201000061.

[26] Y. You, S. Xin, H.Y. Asl, W. Li, P.F. Wang, Y.G. Guo, A. Manthiram, Insights into the improved high-voltage performance of Li-incorporated layered oxide cathodes for sodium-ion batteries, Inside Chem. 4 (2018) 2124–2139, https://doi.org/10.1016/j.chempr.2018.05.018.

[27] P. Zhang, X.D. Li, S. Yu, S.Q. Wu, Z.Z. Zhu, Y. Yang, Effects of Na substitution on Li ion migration in Li 2 CoSiO 4 cathode material, J. Electrochem. Soc. 160 (2013) A658–A661, https://doi.org/10.1149/2.065304jes.

[28] R. El Khalfaouy, A. Addaou, A. Laajeb, A. Lahsini, Synthesis and characterization of Na-substituted LiMnPO4 as a cathode material for improved lithium ion batteries, J. Alloys Compd. 775 (2019) 836–844, https://doi.org/10.1016/j.jallcom.2018.10.161.

[29] P. Xie, Y. Liu, M. Feng, M. Niu, C. Liu, N. Wu, K. Sui, R.R. Patil, D. Pan, Z. Guo, R. Fan, Hierarchically porous Co/C nanocomposites for ultralight high-performance microwave absorption, Adv. Compos. Hybrid Mater. 4 (2021) 173–185, https://doi.org/10.1007/s42114-020-00202-z.

[30] N. Wu, Q. Hu, R. Wei, X. Mai, N. Naik, D. Pan, Z. Guo, Z. Shi, Review on the electromagnetic interference shielding properties of carbon based materials and their novel composites: recent progress, challenges and prospects, Carbon 176 (2021) 88–105, https://doi.org/10.1016/j.carbon.2021.01.124.

[31] Y. Lv, L. Zhu, H. Xu, L. Yang, Z. Liu, D. Cheng, X. Cao, J. Yun, D. Cao, Core/shell template-derived Co, N-doped carbon bifunctional electrocatalysts for rechargeable Zn-air battery, Eng. Sci. (2019), https://doi.org/10.30919/es8d768.

[32] Z. Peng, Q. Jiang, P. Peng, F.-F. Li, NH3-activated fullerene derivative hierarchical microstructures to porous Fe3O4/N-C for oxygen reduction reaction and Zn-air battery, Eng. Sci. (2020), https://doi.org/10.30919/es8d1311.

[33] W. Fan, C. Shan, H. Guo, J. Sang, R. Wang, R. Zheng, K. Sui, Z. Nie, Dual-gradient enabled ultrafast biomimetic snapping of hydrogel materials, Sci. Adv. 5 (2019), https://doi.org/10.1126/sciadv.aav7174.

[34] J. Xu, D.H. Lee, R.J. Clément, X. Yu, M. Leskes, A.J. Pell, G. Pintacuda, X.Q. Yang, C.P. Grey, Y.S. Meng, Identifying the critical role of li substitution in P2-Na x [LiyNizMn1-y-Z]O2 (0 < x, y, z < 1) intercalation cathode materials for high-energy na-ion batteries, Chem. Mater. 26 (2014) 1260–1269, https://doi.org/10.1021/cm403855t.

[35] C. Delmas, J.J. Braconnier, C. Fouassier, P. Hagenmuller, Electrochemical intercalation of sodium in NaxCoO2 bronzes, Solid State Ionics 3–4 (1981) 165–169, https://doi.org/10.1016/0167-2738(81)90076-X.

[36] M. Tamaru, X. Wang, M. Okubo, A. Yamada, Layered Na2RuO3 as a cathode material for Na-ion batteries, Electrochem. Commun. 33 (2013) 23–26, https://doi.org/10.1016/j.elecom.2013.04.011.

[37] P. Rozier, M. Sathiya, A.-R. Paulraj, D. Foix, T. Desaunay, P.-L. Taberna, P. Simon, J.-M. Tarascon, Anionic redox chemistry in Na-rich Na 2 Ru 1−y Sn y O 3 positive electrode material for Na-ion batteries, Electrochem. Commun. 53 (2015) 29–32, https://doi.org/10.1016/j.elecom.2015.02.001.

[38] L. Zheng, H. Wang, M. Luo, G. Wang, Z. Wang, C. Ouyang, Na2MnO3 as cathode materials for Na ion batteries: from first-principles investigations, Solid State Ionics 320 (2018) 210–214, https://doi.org/10.1016/j.ssi.2018.02.039.

[39] E. De La Llave, E. Talaie, E. Levi, P.K. Nayak, M. Dixit, P.T. Rao, P. Hartmann, F. Chesneau, D.T. Major, M. Greenstein, D. Aurbach, L.F. Nazar, Improving energy density and structural stability of manganese oxide cathodes for Na-ion batteries by structural lithium substitution, Chem. Mater. 28 (2016) 9064–9076, https://doi.org/10.1021/acs.chemmater.6b04078.

[40] N. Yabuuchi, R. Hara, M. Kajiyama, K. Kubota, T. Ishigaki, A. Hoshikawa, S. Komaba, New O2/P2-type Li-excess layered manganese oxides as promising multi-functional electrode materials for rechargeable Li/Na batteries, Adv. Energy Mater. 4 (2014) 1301453, https://doi.org/10.1002/aenm.201301453.

[41] P.K. Nayak, J. Grinblat, M. Levi, B. Markovsky, D. Aurbach, Structural and electrochemical evidence of layered to spinel phase transformation of Li and Mn rich layered cathode materials of the formulae xLi[Li 1/3 Mn 2/3]O 2 .(1-x)LiMn 1/3 Ni 1/3 Co 1/3 O 2 (x = 0.2, 0.4, 0.6) upon cycling, J. Electrochem. Soc. 161 (2014) A1534–A1547, https://doi.org/10.1149/2.0101410jes.

[42] R. Berthelot, D. Carlier, C. Delmas, Electrochemical investigation of the P2-NaxCoO2 phase diagram, Nat. Mater. 10 (2011) 74–80, https://doi.org/10.1038/nmat2920.

[43] N. Yabuuchi, M. Kajiyama, J. Iwatate, H. Nishikawa, S. Hitomi, R. Okuyama, R. Usui, Y. Yamada, S. Komaba, P2-type Nax [Fe1/2 Mn1/2]O2 made from earth-abundant elements for rechargeable Na batteries, Nat. Mater. 11 (2012) 512–517, https://doi.org/10.1038/nmat3309.

[44] Z. Lu, J.R. Dahn, Can All the Lithium be Removed from T2-Li[sub 2/3][Ni[sub 1/3]Mn[sub 2/3]]O[sub 2]? J. Electrochem. Soc. 148 (2001) A710, https://doi.org/10.1149/1.1376116.

[45] Z. Lu, J.R. Dahn, In Situ X-Ray Diffraction Study of P2-Na[sub 2/3][Ni[sub 1/3] Mn[sub 2/3]]O[sub 2], J. Electrochem. Soc. 148 (2001) A1225, https://doi.org/10.1149/1.1407247.

[46] Z. Ding, Y. Liu, Q. Tang, Q. Jiang, J. Lu, Z. Xiao, P. Yao, M. Monasterio, J. Wu, X. Liu, Enhanced electrochemical performance of iron-manganese based cathode by Li doping for sodium ion batteries, Electrochim. Acta 292 (2018) 871–878, https://doi.org/10.1016/j.electacta.2018.09.192.

[47] P.F. Wang, Y. You, Y.X. Yin, Y.G. Guo, Layered oxide cathodes for sodium-ion batteries: phase transition, air stability, and performance, Adv. Energy Mater. 8 (2018), https://doi.org/10.1002/aenm.201701912.

[48] L. Yang, X. Li, X. Ma, S. Xiong, P. Liu, Y. Tang, S. Cheng, Y.-Y. Hu, M. Liu, H. Chen, Design of high-performance cathode materials with single-phase pathway for sodium ion batteries: a study on P2-Nax(LiyMn1-y)O2 compounds, J. Power Sources 381 (2018) 171–180, https://doi.org/10.1016/j.jpowsour.2017.12.072.

[49] L. Yang, X. Li, J. Liu, S. Xiong, X. Ma, P. Liu, J. Bai, W. Xu, Y. Tang, Y.Y. Hu, M. Liu, H. Chen, Lithium-doping stabilized high-performance P2-Na0.66Li0.18Fe0.12Mn0.7O2 cathode for sodium ion batteries, J. Am. Chem. Soc. 141 (2019) 6680–6689, https://doi.org/10.1021/jacs.9b01855.

[50] X. Chen, N. Li, E. Kedzie, B.D. McCloskey, H. Tang, W. Tong, High-capacity P2-type Na x Li 0.25 Mn 0.75 O 2 cathode enabled by anionic oxygen redox, J. Electrochem. Soc. 166 (2020) A4136–A4140, https://doi.org/10.1149/2.0611916jes.

[51] Y. Zhu, W. Nie, P. Chen, Y. Zhou, Y. Xu, Li-doping stabilized P2-Li 0.2 Na 1.0 Mn 0.8 O 2 sodium ion cathode with oxygen redox activity, Int. J. Energy Res. 44 (2020) 3253–3259, https://doi.org/10.1002/er.5120.

[52] J. Qiu, B. Chen, H. Hou, X. Wang, X. Liu, L. Ti, T. Liu, R. Chen, S. Wang, B. Li, D. Dai, B. Wang, Improving Na + diffusion and performance of P2-type layered Na 0.6 Li 0.07 Mn 0.66 Co 0.17 Ni 0.17 O 2 by expanding the interplanar spacing, ACS Appl. Mater. Interfaces 12 (2020) 48669–48676, https://doi.org/10.1021/acsami.0c14931.

[53] X.-H. Ma, L.-L. Li, Cheng, F. Qiao, Y.-Y. Ye, N. Li, M.-L. Sha, Z.-F. Zi, J.-M. Dai, P2-type Na0.8(Li0.33Mn0.67-xTix)O2 doped by Ti as cathode materials for high performance sodium-ion batteries, J. Alloys Compd. 815 (2020) 152402, https://doi.org/10.1016/j.jallcom.2019.152402.

[54] B. Zhang, B. Zhang, L. Wang, X. Chen, Y. Lu, B. Xu, W. Yang, Li and Ti Co-doping to stabilize slabs of high-voltage P2-type Na0.560 [Li0.041Mn0.642Ni0.221Ti0.095]O2, J. Alloys Compd. 824 (2020) 153938, https://doi.org/10.1016/j.jallcom.2020.153938.

[55] F.-D. Yu, L.-F. Que, Z.-B. Wang, Y. Zhang, Y. Xue, B.-S. Liu, D.-M. Gu, Layered-spinel capped nanotube assembled 3D Li-rich hierarchitectures for high performance Li-ion battery cathodes, J. Mater. Chem. A. 4 (2016) 18416–18425, https://doi.org/10.1039/C6TA05676H.

[56] Z.Q. Deng, A. Manthiram, Influence of cationic substitutions on the oxygen loss and reversible capacity of lithium-rich layered oxide cathodes, J. Phys. Chem. C 115 (2011) 7097–7103, https://doi.org/10.1021/jp200375d.

[57] S. Komaba, N. Yabuuchi, T. Nakayama, A. Ogata, T. Ishikawa, I. Nakai, Study on the reversible electrode reaction of Na 1-xNi 0.5Mn 0.5O 2 for a rechargeable sodium-ion battery, Inorg. Chem. 51 (2012) 6211–6220, https://doi.org/10.1021/ic300357d.

[58] H. Yu, S. Guo, Y. Zhu, M. Ishida, H. Zhou, Novel titanium-based O3-type NaTi0.5Ni0.5O2 as a cathode material for sodium ion batteries, Chem. Commun. 50 (2014) 457–459, https://doi.org/10.1039/c3cc47351a.

[59] C. Didier, M. Guignard, C. Denage, O. Szajwaj, S. Ito, I. Saadoune, J. Darriet, C. Delmas, Electrochemical Na-deintercalation from NaVO2, Electrochem. Solid State Lett. 14 (2011) A75, https://doi.org/10.1149/1.3555102.

[60] M. Sathiya, K. Hemalatha, K. Ramesha, J.M. Tarascon, A.S. Prakash, Synthesis, structure, and electrochemical properties of the layered sodium insertion cathode material: NaNi 1/3Mn 1/3Co 1/3O 2, Chem. Mater. 24 (2012) 1846–1853, https://doi.org/10.1021/cm300466b.

[61] D. Yuan, X. Hu, J. Qian, F. Pei, F. Wu, R. Mao, X. Ai, H. Yang, Y. Cao, P2-type Na0.67Mn0.65Fe0.2Ni 0.15O2 cathode material with high-capacity for sodium-ion battery, Electrochim. Acta 116 (2014) 300–305, https://doi.org/10.1016/j.electacta.2013.10.211.

[62] N. Yabuchi, M. Kajiyama, J. Iwatate, H. Nishikawa, S. Hitomi, R. Okuyama, R. Usui, Y. Yamada, S. Komaba, P2-type Nax [Fe1/2 Mn1/2[O2 made from earth-abundant elements for rechargeable NaÂ batteries, Nat. Mater. 11 (2012) 512–517, https://doi.org/10.1038/nmat3309.

[63] I. Hasa, D. Buchholz, S. Passerini, B. Scrosati, J. Hassoun, High performance Na0.5[Ni0.23Fe0.13Mn0.63]O2 cathode for sodium-ion batteries, Adv. Energy Mater. 4 (2014), https://doi.org/10.1002/aenm.201400083.

[64] Y. Lu, M. Yanilmaz, C. Chen, Y. Ge, M. Dirican, J. Zhu, Y. Li, X. Zhang, Lithium-substituted sodium layered transition metal oxide fibers as cathodes for sodium-ion batteries, Energy Storage Mater. 1 (2015) 74–81, https://doi.org/10.1016/j.ensm.2015.09.005.

[65] J. Xu, H. Liu, Y.S. Meng, Exploring Li substituted O3-structured layered oxides NaLixNi1/3 - XMn1/3 + xCo1/3 - XO2 (x = 0.07, 0.13, and 0.2) as promising cathode materials for rechargeable Na batteries, Electrochem. Commun. 60 (2015) 13–16, https://doi.org/10.1016/j.elecom.2015.07.023.

[66] N. Voronina, Y.-K. Sun, S.-T. Myung, Co-free layered cathode materials for high energy density lithium-ion batteries, ACS Energy Lett. 5 (2020) 1814–1824, https://doi.org/10.1021/acsenergylett.0c00742.

[67] H. Liu, J. Xu, C. Ma, Y.S. Meng, A new O3-type layered oxide cathode with high energy/power density for rechargeable Na batteries, Chem. Commun. 51 (2015) 4693–4696, https://doi.org/10.1039/c4cc09760b.

[68] M. Ati, L. Dupont, N. Recham, J.N. Chotard, W.T. Walker, C. Davoisne, P. Barpanda, V. Sarou-Kanian, M. Armand, J.M. Tarascon, Synthesis, structural, and transport properties of novel bihydrated fluorosulphates NaMSO4F 2H2O (M=Fe, Co, and Ni), Chem. Mater. 22 (2010) 4062–4068, https://doi.org/10.1021/cm1010482.

[69] L. Mu, S. Xu, Y. Li, Y.S. Hu, H. Li, L. Chen, X. Huang, Prototype sodium-ion batteries using an air-stable and Co/Ni-free O3-layered metal oxide cathode, Adv. Mater. 27 (2015) 6928–6933, https://doi.org/10.1002/adma.201502449.

[70] C. Delmas, C. Fouassier, P. Hagenmuller, Structural classification and properties of the layered oxides, Phys. B+C 99 (1980) 81–85, https://doi.org/10.1016/0378-4363(80)90214-4.

[71] M. Keller, D. Buchholz, S. Passerini, Layered Na-ion cathodes with outstanding performance resulting from the synergetic effect of mixed P- and O-type phases, Adv. Energy Mater. 6 (2016) 1501555, https://doi.org/10.1002/aenm.201501555.

[72] Y. Liu, X. Fang, A. Zhang, C. Shen, Q. Liu, H.A. Enaya, C. Zhou, Layered P2-Na2/3 [Ni1/3Mn2/3]O2 as high-voltage cathode for sodium-ion batteries: the capacity decay mechanism and Al2O3 surface modification, Nano Energy 27 (2016) 27–34, https://doi.org/10.1016/j.nanoen.2016.06.026.

[73] J.L. Yue, Y.N. Zhou, X. Yu, S.M. Bak, X.Q. Yang, Z.W. Fu, O3-type layered transition metal oxide Na(NiCoFeTi)1/4O2 as a high rate and long cycle life cathode material for sodium ion batteries, J. Mater. Chem. A. 3 (2015) 23261–23267, https://doi.org/10.1039/c5ta05769h.

[74] B. Mortemard De Boisse, G. Liu, J. Ma, S.I. Nishimura, S.C. Chung, H. Kiuchi, Y. Harada, J. Kikkawa, Y. Kobayashi, M. Okubo, A. Yamada, Intermediate honeycomb ordering to trigger oxygen redox chemistry in layered battery electrode, Nat. Commun. 7 (2016), https://doi.org/10.1038/ncomms11397.

[75] D.D. Yuan, Y.X. Wang, Y.L. Cao, X.P. Ai, H.X. Yang, Improved electrochemical performance of Fe-substituted NaNi0.5Mn0.5O2 cathode materials for sodium-ion batteries, ACS Appl. Mater. Interfaces 7 (2015) 8585–8591, https://doi.org/10.1021/acsami.5b00594.

[76] Y. Jin, N.J.H. Kneusels, P.C.M.M. Magusin, G. Kim, E. Castillo-Martínez, L. E. Marbella, R.N. Kerber, D.J. Howe, S. Paul, T. Liu, C.P. Grey, Identifying the structural basis for the increased stability of the solid electrolyte interphase formed on silicon with the additive fluoroethylene carbonate, J. Am. Chem. Soc. 139 (2017) 14992–15004, https://doi.org/10.1021/jacs.7b06834.

[77] S.M. Oh, S.T. Myung, J.Y. Hwang, B. Scrosati, K. Amine, Y.K. Sun, High capacity O3-type Na[Li0.05(Ni0.25Fe0.25Mn0.5)0.95]O2 cathode for sodium ion batteries, Chem. Mater. 26 (2014) 6165–6171, https://doi.org/10.1021/cm502481b.

[78] N. Yabuchi, H. Yoshida, S. Komaba, Crystal structures and electrode performance of alpha-NaFeO2 for rechargeable sodium batteries, Electrochemistry 80 (2012) 716–719, https://doi.org/10.5796/electrochemistry.80.716.

[79] J.E. Wang, W.H. Han, K.J. Chang, Y.H. Jung, D.K. Kim, New insight into Na intercalation with Li substitution on alkali site and high performance of O3-type layered cathode material for sodium ion batteries, J. Mater. Chem. A. 6 (2018) 22731–22740, https://doi.org/10.1039/C8TA06159A.

[80] E. Lee, J. Lu, Y. Ren, X. Luo, X. Zhang, J. Wen, D. Miller, A. DeWahl, S. Hackney, B. Key, D. Kim, M.D. Slater, C.S. Johnson, Layered P2/O3 intergrowth cathode: toward high power Na-ion batteries, Adv. Energy Mater. 4 (2014), 1400458, https://doi.org/10.1002/aenm.201400458.

[81] C. Fouassier, C. Delmas, P. Hagenmuller, Evolution structurale et proprietes physiques des phases AXMO2 (A = Na, K; M = Cr, Mn, Co) (x ⩽ 1), Mater. Res. Bull. 10 (1975) 443–449, https://doi.org/10.1016/0025-5408(75)90166-X.

[82] S.P. Ong, V.L. Chevrier, G. Hautier, A. Jain, C. Moore, S. Kim, X. Ma, G. Ceder, Voltage, stability and diffusion barrier differences between sodium-ion and lithium-ion intercalation materials, Energy Environ. Sci. 4 (2011) 3680, https://doi.org/10.1039/c1ee01782a.

[83] L. Yang, J.M.L. Amo, Z. Shadike, S. Bak, F. Bonilla, M. Galceran, P.K. Nayak, J. R. Buchheim, X. Yang, T. Rojo, P. Adelhelm, A Co- and Ni-free P2/O3 biphasic lithium stabilized layered oxide for sodium-ion batteries and its cycling behavior, Adv. Funct. Mater. 30 (2020), https://doi.org/10.1002/adfm.202003364.

[84] S. Guo, P. Liu, H. Yu, Y. Zhu, M. Chen, M. Ishida, H. Zhou, A layered P2- and O3-type composite as a high-energy cathode for rechargeable sodium-ion batteries, Angew. Chem. Int. Ed. 54 (2015) 5894–5899, https://doi.org/10.1002/anie.201411788.

[85] S.P. Guo, J.C. Li, Q.T. Xu, Z. Ma, H.G. Xue, Recent achievements on polyanion-type compounds for sodium-ion batteries: syntheses, crystal chemistry and electrochemical performance, J. Power Sources 361 (2017) 285–299, https://doi.org/10.1016/j.jpowsour.2017.07.002.

[86] U. Nisar, R.A. Shakoor, R. Essehli, R. Amin, B. Orayech, Z. Ahmad, P.R. Kumar, R. Kahraman, S. Al-Qaradawi, A. Soliman, Sodium intercalation/de-intercalation mechanism in Na4MnV(PO4)3 cathode materials, Electrochim. Acta 292 (2018) 98–106, https://doi.org/10.1016/j.electacta.2018.09.111.

[87] H. Kim, R.A. Shakoor, C. Park, S.Y. Lim, J.S. Kim, Y.N. Jo, W. Cho, K. Miyasaka, R. Kahraman, Y. Jung, J.W. Choi, Na2FeP2O7 as a promising iron-based pyrophosphate cathode for sodium rechargeable batteries: a combined experimental and theoretical study, Adv. Funct. Mater. 23 (2013) 1147–1155, https://doi.org/10.1002/adfm.201201589.

[88] R.A. Shakoor, C.S. Park, A.A. Raja, J. Shin, R. Kahraman, A mixed iron-manganese based pyrophosphate cathode, Na2Fe0.5Mn0.5P2O7, for rechargeable sodium ion batteries, Phys. Chem. Chem. Phys. 18 (2016) 3929–3935, https://doi.org/10.1039/c5cp06836c.

[89] Y. Kee, N. Dimov, A. Staikov, P. Barpanda, Y.C. Lu, K. Minami, S. Okada, Insight into the limited electrochemical activity of NaVP2O7, RSC Adv. 5 (2015) 64991–64996, https://doi.org/10.1039/c5ra12158b.

[90] C.A.J. Fisher, V.M.H. Prieto, M.S. Islam, Lithium battery materials LiMPO4 (M = Mn, Fe, Co, and Ni): insights into defect association, transport mechanisms, and doping behavior, Chem. Mater. 20 (2008) 5907–5915, https://doi.org/10.1021/cm801262x.

[91] M.J. Aragón, B. León, T. Serrano, C. Pérez Vicente, J.L. Tirado, Synergistic effects of transition metal substitution in conversion electrodes for lithium-ion batteries, J. Mater. Chem. 21 (2011) 10102–10107, https://doi.org/10.1039/c0jm03880f.

[92] W.R. Liu, Z.Z. Guo, W.S. Young, D.T. Shieh, H.C. Wu, M.H. Yang, N.L. Wu, Effect of electrode structure on performance of Si anode in Li-ion batteries: Si particle size and conductive additive, J. Power Sources 140 (2005) 139–144, https://doi.org/10.1016/j.jpowsour.2004.07.032.

[93] Z. Chen, Y. Qin, K. Amine, Y.K. Sun, Role of surface coating on cathode materials for lithium-ion batteries, J. Mater. Chem. 20 (2010) 7606–7612, https://doi.org/10.1039/c0jm00154f.

[94] J.J. Abraham, H. Tariq, R.A. Shakoor, R. Kahraman, S. Al-Qaradawi, Synthesis and performance evaluation of Na (2-x) Li x FeP 2 O7 (x=0, 0.6) hybrid cathodes, ChemistrySelect 5 (2020) 12548–12557, https://doi.org/10.1002/slct.202003658.

[95] K. Ozawa, Lithium-ion rechargeable batteries with LiCoO2 and carbon electrodes: the LiCoO2/C system, Solid State Ionics 69 (1994) 212–221, https://doi.org/10.1016/0167-2738(94)90411-1.

[96] D. Arumugam, G.P. Kalaignan, P. Manisankar, Development of structural stability and the electrochemical performances of "La" substituted spinel LiMn2O4 cathode materials for rechargeable lithium-ion batteries, Solid State Ionics 179 (2008) 580–586, https://doi.org/10.1016/j.ssi.2008.04.010.

[97] S.H. Park, Y. Sato, J.K.K. Kim, Y.S. Lee, Powder property and electrochemical characterization of Li2MnO3 material, Mater. Chem. Phys. 102 (2007) 225–230, https://doi.org/10.1016/j.matchemphys.2006.12.008.

[98] D.Y.W. Yu, K. Yanagida, Y. Kato, H. Nakamura, Electrochemical Activities in Li [sub 2]MnO[sub 3], J. Electrochem. Soc. 156 (2009) A417, https://doi.org/10.1149/1.3110803.

[99] S. Francis Amalraj, B. Markovsky, D. Sharon, M. Talianker, E. Zinigrad, R. Persky, O. Haik, J. Grinblat, J. Lampert, M. Schulz-Dobrick, A. Garsuch, L. Burlaka, D. Aurbach, Study of the electrochemical behavior of the "inactive" Li 2MnO 3, Electrochim. Acta 78 (2012) 32–39, https://doi.org/10.1016/j.electacta.2012.05.144.

[100] H.A. Tariq, J.J. Abraham, R.A. Shakoor, S. Al-Qaradawi, M.R. Abdul Karim, U. Chaudhry, Synthesis of lithium manganese oxide nanocomposites using microwave-assisted chemical precipitation technique and their performance evaluation in lithium-ion batteries, Energy Storage 2 (2020), https://doi.org/10.1002/est2.202.

[101] V. Massarotti, D. Capsoni, M. Bini, G. Chiodelli, C.B. Azzoni, M.C. Mozzati, A. Paleari, Electric and magnetic properties of LiMn2O4- and Li2MnO3-type oxides, J. Solid State Chem. 131 (1997) 94–100, https://doi.org/10.1006/jssc.1997.7349.

[102] Y. Okamoto, Ambivalent effect of oxygen vacancies on Li 2 MnO 3 : a first-principles study, J. Electrochem. Soc. 159 (2011) A152–A157, https://doi.org/10.1149/2.079202jes.

[103] G.G. Amatucci, N. Pereira, T. Zheng, J.-M. Tarascon, Failure Mechanism and Improvement of the Elevated Temperature Cycling of LiMn[sub 2]O[sub 4] Compounds through the Use of the LiAl[sub x]Mn[sub 2−x]O[sub 4−z]F[sub z] Solid Solution, J. Electrochem. Soc. 148 (2001) A171, https://doi.org/10.1149/1.1342168.

[104] T. Aoshima, K. Okahara, C. Kiyohara, K. Shizuka, Mechanisms of manganese spinels dissolution and capacity fade at high temperature, in: J. Power Sources

(Ed.), Elsevier, 2001, pp. 377–380, https://doi.org/10.1016/S0378-7753(01)00551-1.

[105] A. Du Pasquier, A. Blyr, A. Cressent, C. Lenain, G. Amatucci, J.M. Tarascon, An update on the high temperature ageing mechanism in LiMn2O4-based Li-ion cells, J. Power Sources 81–82 (1999) 54–59, https://doi.org/10.1016/S0378-7753(99)00136-6.

[106] M. Tabuchi, Y. Nabeshima, T. Takeuchi, H. Kageyama, K. Tatsumi, J. Akimoto, H. Shibuya, J. Imaizumi, Synthesis and electrochemical characterization of Fe and Ni substituted Li2MnO3 - an effective means to use Fe for constructing "co-free" Li2MnO3 based positive electrode material, J. Power Sources 196 (2011) 3611–3622, https://doi.org/10.1016/j.jpowsour.2010.12.060.

[107] M. Tabuchi, Y. Nabeshima, T. Takeuchi, K. Tatsumi, J. Imaizumi, Y. Nitta, Fe content effects on electrochemical properties of Fe-substituted Li2MnO3 positive electrode material, J. Power Sources 195 (2010) 834–844, https://doi.org/10.1016/j.jpowsour.2009.08.059.

[108] H.J. Guo, X.Q. Li, F.Y. He, X.H. Li, Z.X. Wang, W.J. Peng, Effects of sodium substitution on properties of LiMn2O 4 cathode for lithium ion batteries, Trans. Nonferrous Met. Soc. China 20 (2010) 1043–1048, https://doi.org/10.1016/S1003-6326(09)60255-7.

[109] R.D. Shannon, Revised effective ionic radii and systematic studies of interatomic distances in halides and chalcogenides, Acta Crystallogr. Sect. A (1976), https://doi.org/10.1107/S0567739476001551.

[110] X. Dong, Y. Xu, L. Xiong, X. Sun, Z. Zhang, Sodium substitution for partial lithium to significantly enhance the cycling stability of Li2MnO3 cathode material, J. Power Sources 243 (2013) 78–87, https://doi.org/10.1016/j.jpowsour.2013.05.155.

[111] M. Wood, J.L. Li, R.E. Ruther, Z. Du, E.C. Self, H.M. Meyer, C. Daniel, I. Belharouak, D.L. Wood, Chemical stability and long-term cell performance of low-cobalt, Ni-Rich cathodes prepared by aqueous processing for high-energy Li-Ion batteries, Energy Storage Mater 24 (2020) 188–197, https://doi.org/10.1016/j.ensm.2019.08.020.

[112] K.J. Park, J.Y. Hwang, H.H. Ryu, F. Maglia, S.J. Kim, P. Lamp, C.S. Yoon, Y. K. Sun, Degradation mechanism of Ni-enriched NCA cathode for lithium batteries: are microcracks really critical? ACS Energy Lett. 4 (2019) 1394–1400, https://doi.org/10.1021/acsenergylett.9b00733.

[113] P. Zhou, H. Meng, Z. Zhang, C. Chen, Y. Lu, J. Cao, F. Cheng, J. Chen, Stable layered Ni-rich LiNi0.9Co0.07Al0.03O2 microspheres assembled with nanoparticles as high-performance cathode materials for lithium-ion batteries, J. Mater. Chem. A 5 (2017) 2724–2731, https://doi.org/10.1039/c6ta09921a.

[114] H.J. Noh, S. Youn, C.S. Yoon, Y.K. Sun, Comparison of the structural and electrochemical properties of layered Li[NixCoyMnz]O2 (x = 1/3, 0.5, 0.6, 0.7, 0.8 and 0.85) cathode material for lithium-ion batteries, J. Power Sources 233 (2013) 121–130, https://doi.org/10.1016/j.jpowsour.2013.01.063.

[115] B.B. Lim, S.T. Myung, C.S. Yoon, Y.K. Sun, Comparative study of Ni-rich layered cathodes for rechargeable lithium batteries: Li[Ni0.85Co0.11Al0.04]O2 and Li[Ni0.84Co0.06Mn0.09Al0.01]O2 with two-step full concentration gradients, ACS Energy Lett. 1 (2016) 283–289, https://doi.org/10.1021/acsenergylett.6b00150.

[116] H.H. Ryu, K.J. Park, C.S. Yoon, Y.K. Sun, Capacity fading of ni-rich li[NixCoyMn1-x-y]O2 (0.6 ≤ x ≤ 0.95) cathodes for high-energy-density lithium-ion batteries: bulk or surface degradation? Chem. Mater. 30 (2018) 1155–1163, https://doi.org/10.1021/acs.chemmater.7b05269.

[117] C.S. Yoon, M.H. Choi, B.-B. Lim, E.-J. Lee, Y.-K. Sun, Review—high-capacity Li[Ni1- x Co x/2 Mn x/2]O 2 (x = 0.1, 0.05, 0) cathodes for next-generation Li-ion battery, J. Electrochem. Soc. 162 (2015) A2483–A2489, https://doi.org/10.1149/2.0101514jes.

[118] W. Liu, P. Oh, X. Liu, M.J. Lee, W. Cho, S. Chae, Y. Kim, J. Cho, Nickel-rich layered lithium transition-metal oxide for high-energy lithium-ion batteries, Angew. Chem. Int. Ed. 54 (2015) 4440–4457, https://doi.org/10.1002/anie.201409262.

[119] C. Fu, G. Li, D. Luo, Q. Li, J. Fan, L. Li, Nickel-rich layered microspheres cathodes: lithium/nickel disordering and electrochemical performance, ACS Appl. Mater. Interfaces 6 (2014) 15822–15831, https://doi.org/10.1021/am5030726.

[120] H. Xie, K. Du, G. Hu, Z. Peng, Y. Cao, The role of sodium in LiNi0.8Co0.15Al0.05O2 cathode material and its electrochemical behaviors, J. Phys. Chem. C 120 (2016) 3235–3241, https://doi.org/10.1021/acs.jpcc.5b12407.

[121] Z. Huang, Z. Wang, Q. Jing, H. Guo, X. Li, Z. Yang, Investigation on the effect of Na doping on structure and Li-ion kinetics of layered LiNi0.6Co0.2Mn0.2O2 cathode material, Electrochim. Acta 192 (2016) 120–126, https://doi.org/10.1016/j.electacta.2016.01.139.

[122] W. Hua, J. Zhang, Z. Zheng, W. Liu, X. Peng, X.D. Guo, B. Zhong, Y.J. Wang, X. Wang, Na-doped Ni-rich LiNi0.5Co0.2Mn0.3O2 cathode material with both high rate capability and high tap density for lithium ion batteries, Dalt. Trans. 43 (2014) 14824–14832, https://doi.org/10.1039/c4dt01611d.

[123] C. Gong, W. Lv, L. Qu, O.E. Bankole, G. Li, R. Zhang, M. Hu, L. Lei, Syntheses and electrochemical properties of layered Li 0.95Na0.05Ni1/3Co1/3Mn 1/3O2 and LiNi1/3Co1/3Mn 1/3O2, J. Power Sources 247 (2014) 151–155, https://doi.org/10.1016/j.jpowsour.2013.08.081.

[124] W. He, D. Yuan, J. Qian, X. Ai, H. Yang, Y. Cao, Enhanced high-rate capability and cycling stability of Na-stabilized layered Li1.2[Co0.13Ni0.13Mn0.54]O2 cathode material, J. Mater. Chem. A. 1 (2013) 11397, https://doi.org/10.1039/c3ta12296d.

[125] Y. Su, F. Yuan, L. Chen, Y. Lu, J. Dong, Y. Fang, S. Chen, F. Wu, Enhanced high-temperature performance of Li-rich layered oxide via surface heterophase coating, J. Energy Chem. 51 (2020) 39–47, https://doi.org/10.1016/j.jechem.2020.03.033.

[126] J. Wang, X. He, E. Paillard, N. Laszczynski, J. Li, S. Passerini, Lithium- and manganese-rich oxide cathode materials for high-energy lithium ion batteries, Adv. Energy Mater. 6 (2016), https://doi.org/10.1002/aenm.201600906.

[127] J. Zhao, R. Huang, W. Gao, J.-M. Zuo, X.F. Zhang, S.T. Misture, Y. Chen, J. V. Lockard, B. Zhang, S. Guo, M.R. Khoshi, K. Dooley, H. He, Y. Wang, An ion-exchange promoted phase transition in a Li-excess layered cathode material for high-performance lithium ion batteries, Adv. Energy Mater. 5 (2015), https://doi.org/10.1002/aenm.201401937.

[128] N. Yabuuchi, K. Yoshii, S.T. Myung, I. Nakai, S. Komaba, Detailed studies of a high-capacity electrode material for rechargeable batteries, Li2MnO3-LiCo1/3Ni 1/3Mn1/3O2, J. Am. Chem. Soc. 133 (2011) 4404–4419, https://doi.org/10.1021/ja108588y.

[129] U. Nisar, R. Amin, A. Shakoor, R. Essehli, S. Al-Qaradawi, R. Kahraman, I. Belharouak, Synthesis and electrochemical characterization of Cr-doped lithium-rich Li1.2Ni0.16Mn0.56Co0.08-xCrxO2 cathodes, Emergent Mater 1 (2018) 155–164, https://doi.org/10.1007/s42247-018-0014-0.

[130] S. Zhang, J. Chen, T. Tang, Y. Jiang, G. Chen, Q. Shao, C. Yan, T. Zhu, M. Gao, Y. Liu, H. Pan, A novel strategy to significantly enhance the initial voltage and suppress voltage fading of a Li- and Mn-rich layered oxide cathode material for lithium-ion batteries, J. Mater. Chem. A 6 (2018) 3610–3624, https://doi.org/10.1039/c7ta10887g.

[131] R. Shunmugasundaram, R. Senthil Arumugam, J.R. Dahn, High capacity li-rich positive electrode materials with reduced first-cycle irreversible capacity loss, Chem. Mater. 27 (2015) 757–767, https://doi.org/10.1021/cm504583y.

[132] G. Assat, D. Foix, C. Delacourt, A. Iadecola, R. Dedryvère, J.M. Tarascon, Fundamental interplay between anionic/cationic redox governing the kinetics and thermodynamics of lithium-rich cathodes, Nat. Commun. 8 (2017) 1–12, https://doi.org/10.1038/s41467-017-02291-9.

[133] U. Nisar, R. Petla, S.A. Jassim Al-Hail, A.A. Quddus, H. Monawwar, A. Shakoor, R. Essehli, R. Amin, Impact of surface coating on electrochemical and thermal behaviors of a Li-rich Li1.2Ni0.16Mn0.56Co0.08O2 cathode, RSC Adv. 10 (2020) 15274–15281, https://doi.org/10.1039/d0ra02060e.

[134] J. James Abraham, U. Nisar, H. Monawwar, A. Abdul Quddus, R.A. Shakoor, M. I. Saleh, R. Kahraman, S. Al-Qaradawi, A.S. Aljaber, Improved electrochemical performance of SiO2-coated Li-rich layered oxides-Li1.2Ni0.13Mn0.54Co0.13O2, J. Mater. Sci. Mater. Electron. (2020) 1–12, https://doi.org/10.1007/s10854-020-04481-6.

[135] Y. Wang, L. Wang, X. Guo, T. Wu, Y. Yang, B. Wang, E. Wang, H. Yu, Thermal stability enhancement through structure modification on the microsized crystalline grain surface of lithium-rich layered oxides, ACS Appl. Mater. Interfaces 12 (2020) 8306–8315, https://doi.org/10.1021/acsami.9b21303.

[136] V. Hebbar, M. Viji, A.K. Budumuru, S. Gautam, K.H. Chae, K. Balaji, N.T. Kalyana Sundaram, A.K. Subramani, C. Sudakar, Morphology and interconnected microstructure-driven high-rate capability of Li-rich layered oxide cathodes, ACS Appl. Mater. Interfaces 12 (2020) 32566–32577, https://doi.org/10.1021/acsami.0c05752.

[137] Z. Yu, F. Ning, B. Li, Z. Sun, W. Chu, D. Xia, Mitigating voltage decay of Li-rich layered oxide by incorporation of 5d metal rhenium, J. Phys. Chem. C 123 (2019) 18870–18876, https://doi.org/10.1021/acs.jpcc.9b05683.

[138] S. Jamil, R. Yu, Q. Wang, M. Fasehullah, Y. Huang, Z. Yang, X. Yang, X. Wang, Enhanced cycling stability of nickel-rich layered oxide by tantalum doping, J. Power Sources 473 (2020), https://doi.org/10.1016/j.jpowsour.2020.228597.

[139] M.J. Wang, F. Da Yu, G. Sun, J. Wang, J.G. Zhou, D.M. Gu, Z.B. Wang, Co-regulating the surface and bulk structure of Li-rich layered oxides by a phosphor doping strategy for high-energy Li-ion batteries, J. Mater. Chem. A 7 (2019) 8302–8314, https://doi.org/10.1039/c9ta00783k.

[140] B. Xu, C.R. Fell, M. Chi, Y.S. Meng, Identifying surface structural changes in layered Li-excess nickel manganese oxides in high voltage lithium ion batteries: a joint experimental and theoretical study, Energy Environ. Sci. 4 (2011) 2223, https://doi.org/10.1039/c1ee01131f.

[141] S. Chen, Z. Chen, M. Xia, C. Cao, Y. Luo, Toward alleviating voltage decay by sodium substitution in lithium-rich manganese-based oxide cathodes, ACS Appl. Energy Mater. 1 (2018) 4065–4074, https://doi.org/10.1021/acsaem.8b00740.

[142] J. Reed, G. Ceder, A. Van Der Ven, Layered-to-Spinel Phase Transition in Li[sub x] MnO[sub 2], Electrochem. Solid State Lett. 4 (2001) A78, https://doi.org/10.1149/1.1368896.

[143] Z. Xue, X. Qi, L. Li, W. Li, L. Xu, Y. Xie, X. Lai, G. Hu, Z. Peng, Y. Cao, K. Du, Sodium doping to enhance electrochemical performance of overlithiated oxide cathode materials for Li-ion batteries via Li/Na ion-exchange method, ACS Appl. Mater. Interfaces 10 (2018) 27141–27149, https://doi.org/10.1021/acsami.8b10178.

[144] Y. Hu, Z. Qin, J. Pei, B. Cong, X. Yang, G. Chen, Reduced lithium/nickel disorder degree of sodium-doped lithium-rich layered oxides for cathode materials: experiments and calculations, ChemElectroChem 7 (2020) 246–251, https://doi.org/10.1002/celc.201901846.

[145] W. He, D. Yuan, J. Qian, X. Ai, H. Yang, Y. Cao, Enhanced high-rate capability and cycling stability of Na-stabilized layered Li1.2[Co0.13Ni0.13Mn 0.54]O2 cathode material, J. Mater. Chem. A 1 (2013) 11397–11403, https://doi.org/10.1039/c3ta12296d.

[146] B. Qiu, J. Wang, Y. Xia, Y. Liu, L. Qin, X. Yao, Z. Liu, Effects of Na+ contents on electrochemical properties of Li 1.2Ni0.13Co0.13Mn0.54O2 cathode materials, J. Power Sources 240 (2013) 530–535, https://doi.org/10.1016/j.jpowsour.2013.04.047.

[147] S.H. Park, S.S. Shin, Y.K. Sun, The effects of Na doping on performance of layered Li 1.1 - XNax[Ni0.2Co0.3Mn 0.4]O2 materials for lithium secondary batteries,

Mater. Chem. Phys. 95 (2006) 218–221, https://doi.org/10.1016/j.matchemphys.2005.06.014.

[148] S.N. Lim, J.Y. Seo, D.S. Jung, W. Ahn, H.S. Song, S.H. Yeon, S. Bin Park, Rate capability for Na-doped Li1.167Ni0.18Mn0.548Co0.105O2 cathode material and characterization of Li-ion diffusion using galvanostatic intermittent titration technique, J. Alloys Compd. 623 (2015) 55–61, https://doi.org/10.1016/j.jallcom.2014.09.203.

[149] C. Yang, X. Zhang, J. Huang, P. Ao, G. Zhang, Enhanced rate capability and cycling stability of Li1.2-xNaxMn0.54Co0.13Ni0.13O2, Electrochim. Acta 196 (2016) 261–269, https://doi.org/10.1016/j.electacta.2016.02.180.

[150] E. Han, Q. Jing, L. Zhu, G. Zhang, S. Ma, The effects of sodium additive on Li1.17Ni0.10Co0.10Mn0.63O32for lithium ion batteries, J. Alloys Compd. 618 (2015) 629–634, https://doi.org/10.1016/j.jallcom.2014.08.220.

[151] R.P. Qing, J.L. Shi, D.D. Xiao, X.D. Zhang, Y.X. Yin, Y.B. Zhai, L. Gu, Y.G. Guo, Enhancing the kinetics of Li-rich cathode materials through the pinning effects of gradient surface Na+ doping, Adv. Energy Mater. 6 (2016), https://doi.org/10.1002/aenm.201501914.

[152] X. Yin, K. Huang, S. Liu, H. Wang, H. Wang, Preparation and characterization of Na-doped LiFePO4/C composites as cathode materials for lithium-ion batteries, J. Power Sources 195 (2010) 4308–4312, https://doi.org/10.1016/j.jpowsour.2010.01.019.

[153] A.K. Padhi, K.S. Nanjundaswamy, C. Masquelier, S. Okada, J.B. Goodenough, Effect of structure on the Fe3 +/Fe2 + redox couple in iron phosphates, J. Electrochem. Soc. 144 (1997) 1609–1613, https://doi.org/10.1149/1.1837649.

[154] M. Zhong, Z. Zhou, Effect of reactant phase form on the properties of LiFePO4 synthesized by carbothermal reduction method, Solid State Ionics 181 (2010) 1607–1610, https://doi.org/10.1016/j.ssi.2010.09.015.

[155] X. Yang, Z. Hu, J. Liang, Effects of sodium and vanadium co-doping on the structure and electrochemical performance of LiFePO4/C cathode material for lithium-ion batteries, Ceram. Int. 41 (2015) 2863–2868, https://doi.org/10.1016/j.ceramint.2014.10.108.

[156] C.Y. Ouyang, S.Q. Shi, Z.X. Wang, H. Li, X.J. Huang, L.Q. Chen, The effect of Cr doping on Li ion diffusion in LiFePO 4 from first principles investigations and Monte Carlo simulations, J. Phys. Condens. Matter 16 (2004) 2265–2272, https://doi.org/10.1088/0953-8984/16/13/007.

[157] X. Xin, H. Li, Q. Chang, W. Wang, Preparation and investigation on lattice distortion and electrochemical performances of Li 0.95 Na 0.05 FePO 4/C, Chinese, J. Chem. Phys. 25 (2012) 429–433, https://doi.org/10.1088/1674-0068/25/04/429-433.

[158] J. Zhang, S.-H. Luo, Q.-X. Ren, D.-J. Zhang, Y. Qin, Tailoring the sodium doped LiMnPO4/C orthophosphate to nanoscale as a high-performance cathode for lithium ion battery, Appl. Surf. Sci. 530 (2020) 146628, https://doi.org/10.1016/j.apsusc.2020.146628.

[159] J. Li, S. Luo, Y. Sun, J. Li, J. Zhang, T.-F. Yi, Li0.95Na0.05MnPO4/C nanoparticles compounded with reduced graphene oxide sheets for superior lithium ion battery cathode performance, Ceram. Int. 45 (2019) 4849–4856, https://doi.org/10.1016/j.ceramint.2018.11.181.

[160] I. Nakai, K. Takahashi, Y. Shiraishi, T. Nakagome, F. Nishikawa, Study of the Jahn–Teller distortion in LiNiO2, a cathode material in a rechargeable lithium battery, byin SituX-ray absorption fine structure analysis, J. Solid State Chem. 140 (1998) 145–148, https://doi.org/10.1006/jssc.1998.7943.

[161] Y. Hong, Z. Tang, Z. Zhang, Enhanced electrochemical properties of LiMnPO4/C composites by tailoring polydopamine-derived carbon coating, Electrochim. Acta 176 (2015) 369–377, https://doi.org/10.1016/j.electacta.2015.07.018.

[162] Q. Hu, J.-Y. Liao, B.-K. Zou, M.-F. Yu, Z.-F. Tang, Z.-Y. Wen, C.-H. Chen, Improving the rate and low-temperature performance of LiFePO4 by tailoring the form of carbon coating from amorphous to graphene-like, J. Solid State Electrochem. 22 (2018) 797–805, https://doi.org/10.1007/s10008-017-3777-y.

[163] R. Wanga, S. Xiao, X. Li, J. Wang, H. Guo, F. Zhong, Structural and electrochemical performance of Na-doped Li3V2(PO4)3/C cathode materials for lithium-ion batteries via rheological phase reaction, J. Alloys Compd. 575 (2013) 268–272, https://doi.org/10.1016/j.jallcom.2013.03.276.

[164] M.Y. Saïdi, J. Barker, H. Huang, J.L. Swoyer, G. Adamson, Performance characteristics of lithium vanadium phosphate as a cathode material for lithium-ion batteries, J. Power Sources 119–121 (2003) 266–272, https://doi.org/10.1016/S0378-7753(03)00245-3.

[165] M. Liu, X. Guo, Synthesis and performance of Li3V2(PO4)3/C composites as cathode materials, Rare Met. 27 (2008) 571–574.

[166] Q. Kuang, Y. Zhao, Z. Liang, Synthesis and electrochemical properties of Na-doped Li3V 2(PO4)3 cathode materials for Li-ion batteries, J. Power Sources 196 (2011) 10169–10175, https://doi.org/10.1016/j.jpowsour.2011.08.044.

[167] Y. Xu, X. Han, L. Zheng, W. Yan, Y. Xie, Pillar effect on cyclability enhancement for aqueous lithium ion batteries: a new material of β-vanadium bronze M0.33V2O5 (M = Ag{,} Na) nanowires, J. Mater. Chem. 21 (2011) 14466–14472, https://doi.org/10.1039/C1JM11910A.

[168] P. Li, L. Shao, P. Wang, X. Zheng, H. Yu, S. Qian, M. Shui, N. Long, J. Shu, Lithium sodium vanadium phosphate and its phase transition as cathode material for lithium ion batteries, Electrochim. Acta 180 (2015) 120–128, https://doi.org/10.1016/j.electacta.2015.08.115.

[169] W. Mao, Y. Ma, S. Liu, Z. Tang, Y. Fu, Facile Synthesis of hybrid phase Li2NaV2 (PO4)3 and its application in lithium ion full cell: Li2NaV2(PO4)3|| Li2NaV2 (PO4)3, Electrochim. Acta 147 (2014) 498–505, https://doi.org/10.1016/j.electacta.2014.09.148.

[170] S.Q. Wu, Z.Z. Zhu, Y. Yang, Z.F. Hou, Effects of Na-substitution on structural and electronic properties of Li2CoSiO4 cathode material, Trans. Nonferrous Met. Soc. China 19 (2009) 182–186, https://doi.org/10.1016/S1003-6326(08)60249-6.

[171] M. Wang, M. Yang, L. Ma, X. Shen, Synthesis and improved electrochemical properties of Na-substituted Li2MnSiO4 nanoparticles as cathode materials for Li-ion batteries, Chem. Phys. Lett. 619 (2015) 39–43, https://doi.org/10.1016/j.cplett.2014.11.025.

[172] L. Xiong, Y. Xu, P. Lei, T. Tao, X. Dong, J. Song, The electrochemical performance of sodium-ion-modified spinel LiMn 2O4 used for lithium-ion batteries, J. Solid State Electrochem. 18 (2014) 713–719, https://doi.org/10.1007/s10008-013-2307-9.

[173] J. Wang, W. Lin, B. Wu, J. Zhao, Syntheses and electrochemical properties of the Na-doped LiNi0.5Mn1.5O4 cathode materials for lithium-ion batteries, Electrochim. Acta 145 (2014) 245–253, https://doi.org/10.1016/j.electacta.2014.07.140.

[174] Z. Liu, Y. Fan, W. Peng, Z. Wang, H. Guo, X. Li, J. Wang, Mechanical activation assisted soft chemical synthesis of Na-doped lithium vanadium fluorophosphates with improved lithium storage properties, Ceram. Int. 41 (2015) 4267–4271, https://doi.org/10.1016/j.ceramint.2014.11.097.

[175] B.L. Ellis, K.T. Lee, L.F. Nazar, Positive electrode materials for Li-Ion and Li-batteries, Chem. Mater. 22 (2010) 691–714, https://doi.org/10.1021/cm902696j.

[176] J.B. Goodenough, Y. Kim, Challenges for rechargeable Li batteries, Chem. Mater. 22 (2010) 587–603, https://doi.org/10.1021/cm901452z.

[177] J.M. Tarascon, M. Armand, Issues and challenges facing rechargeable lithium batteries, Nature 414 (2001) 359–367, https://doi.org/10.1038/35104644.

[178] Y. Liu, D. He, R. Han, G. Wei, Y. Qiao, Nanostructured potassium and sodium ion incorporated Prussian blue frameworks as cathode materials for sodium-ion batteries, Chem. Commun. 53 (2017) 5569–5572, https://doi.org/10.1039/c7cc02303k.

[179] J. Zhang, Y. Lai, P. Li, Y. Wang, F. Zhong, X. Feng, W. Chen, J. Liu, X. Ai, H. Yang, Y. Cao, Boosting rate and cycling performance of K-doped Na3V2(PO4)2F3 cathode for high-energy-density sodium-ion batteries, Green Energy Environ. (2021), https://doi.org/10.1016/j.gee.2021.01.001.

[180] Y. Cao, Y. Liu, D. Zhao, J. Zhang, X. Xia, T. Chen, L. chang Zhang, P. Qin, Y. Xia, K-doped Na3Fe2(PO4)3 cathode materials with high-stable structure for sodium-ion stored energy battery, J. Alloys Compd. 784 (2019) 939–946, https://doi.org/10.1016/j.jallcom.2019.01.125.

[181] K. Wang, Z.G. Wu, T. Zhang, Y.P. Deng, J.T. Li, X.D. Guo, B. Bin Xu, B.H. Zhong, P2-type Na0.67Mn0.72Ni0.14Co0.14O2 with K+ doping as new high rate performance cathode material for sodium-ion batteries, Electrochim. Acta 216 (2016) 51–57, https://doi.org/10.1016/j.electacta.2016.09.003.

[182] Z. Liu, Z. Zhang, Y. Liu, L. Li, S. Fu, Facile and scalable fabrication of K + -doped Li 1.2 Ni 0.2 Co 0.08 Mn 0.52 O 2 cathode with ultra high capacity and enhanced cycling stability for lithium ion batteries, Solid State Ionics 332 (2019) 47–54, https://doi.org/10.1016/j.ssi.2018.12.021.

[183] J. Zhao, Z. Wang, J. Wang, H. Guo, X. Li, W. Gui, N. Chen, G. Yan, Anchoring K + in Li + sites of LiNi 0.8 Co 0.15 Al 0.05 O 2 cathode material to suppress its structural degradation during high-voltage cycling, Energy Technol. 6 (2018) 2358–2366, https://doi.org/10.1002/ente.201800361.

[184] Y. Wang, Z. Feng, P. Cui, W. Zhu, Y. Gong, M.A. Girard, G. Lajoie, J. Trottier, Q. Zhang, L. Gu, Y. Wang, W. Zuo, Y. Yang, J.B. Goodenough, K. Zaghib, Pillar-beam structures prevent layered cathode materials from destructive phase transitions, Nat. Commun. 12 (2021) 1–11, https://doi.org/10.1038/s41467-020-20169-1.

[185] A. Das, S.B. Majumder, A. Roy Chaudhuri, K+ and Mg2+ co-doped bipolar Na3V2 (PO4)3: an ultrafast electrode for symmetric sodium ion full cell, J. Power Sources 461 (2020), https://doi.org/10.1016/j.jpowsour.2020.228149.